Supporting Information for

Screening and investigation of a cyanine fluorescence probe for simultaneous sensing of glutathione and cysteine with single excitation

Xu Wang, Jianzheng Lv, Xueying Yao, Yong Li, Fang Huang, Mengmeng Li, Jie Yang, Xiuyun Ruan, Bo Tang*

College of Chemistry, Chemical Engineering and Materials Science, Collaborative Innovation Center of Functionalized Probes for Chemical Imaging, Key Laboratory of Molecular and Nano Probes, Ministry of Education, Shandong Normal University, Jinan 250014, P. R. China

* Corresponding author. Tel.: +86-531-86180010; Fax: +86-531-86180017.

E-mail address: tangb@sdnu.edu.cn (B. Tang).

Contents

Part I

Part II

Part I

1. Enlarged figures and tables in the main manuscript

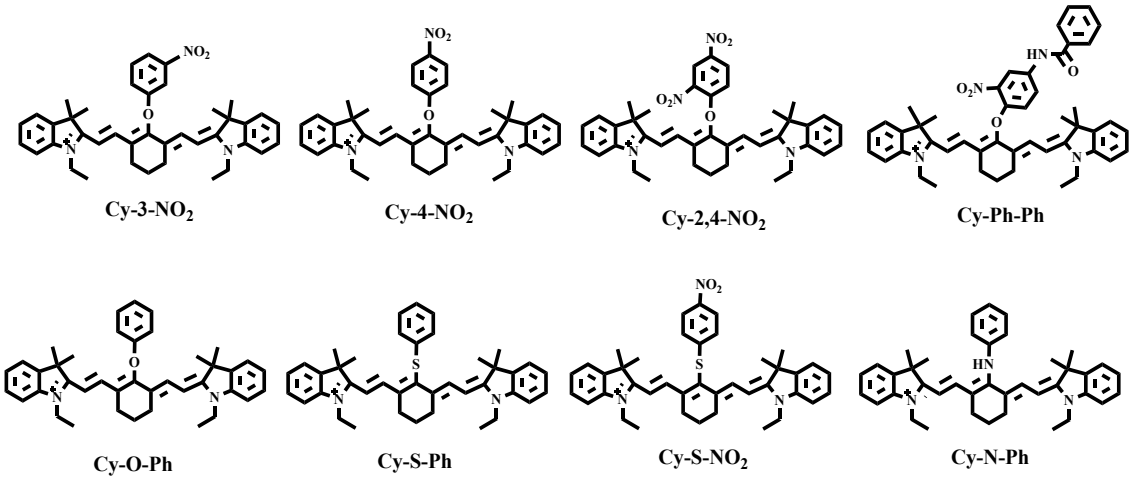

Figure 1 Molecular structures of synthesized dyes.

Table 1 Photophysical properties of the synthesized dyes

Dyes	[a]abs$_{max}$/nm	[a]Ex$_{max}$/nm	[a]Em$_{max}$/nm	[a]Extinction coefficient /10^4 M^{-1} cm^{-1}	[a]Stokes shift/nm	[b]Φ_{fl} ($\times10^2$)
Cy-O-Ph	760	764	786	7.39	22	10.3
Cy-3-NO_2	765	763	786	5.66	23	0.41
Cy-4-NO_2	765	765	788	7.85	23	2.0
Cy-2,4-NO_2	763	740	760	3.90	20	1.60
Cy-Ph-Ph	710,783	763	783	3.68	20	0.03
Cy-S-Ph	783	780	805	6.89	25	0.76
Cy-S-NO_2	788	785	806	4.02	21	0.36
Cy-N-Ph	739	735	780	2.40	44	1.50
Cy-Cys	788	734	754	1.54	20	2.60
Cy-Hcy	787	773	797	1.76	24	0.45
Cy-GSH	782	780	806	10.1	26	4.30

[a]Measured in 50 mM phosphate buffer (pH 7.4, 1% CH_3CN). [b]$\Phi_{fl}$is the relative fluorescence quantum yield estimated by using ICG (Φ=0.13[9]) as a fluorescence standard.

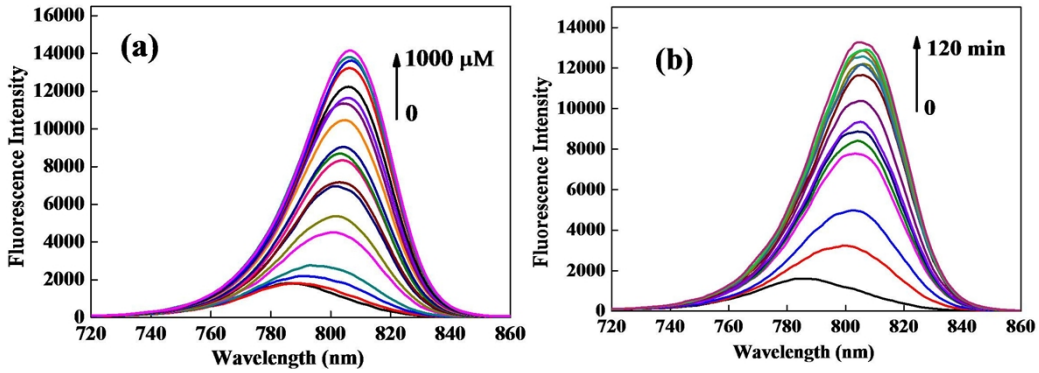

Figure 2 FS variation of Cy-3-NO_2 (10 μM) in the presence of GSH. (a) The FS recorded after Cy-3-NO_2 reacted with 0, 2.5, 5, 10, 20, 30, 40, 50, 60, 70, 80, 90, 100, 200, 300, 400, 500, 700, 900, and 1000 μM GSH for 2h. (b) The FS recorded after Cy-3-NO_2 reacted with GSH (500 μM) for 0, 2.5, 5, 10, 15, 20, 25, 30, 45, 60, 70, 90, 100, 110, and 120 min. λ_{ex}=710 nm, 50 mM PBS buffer (pH=7.4, 1% CH_3CN), 37 °C.

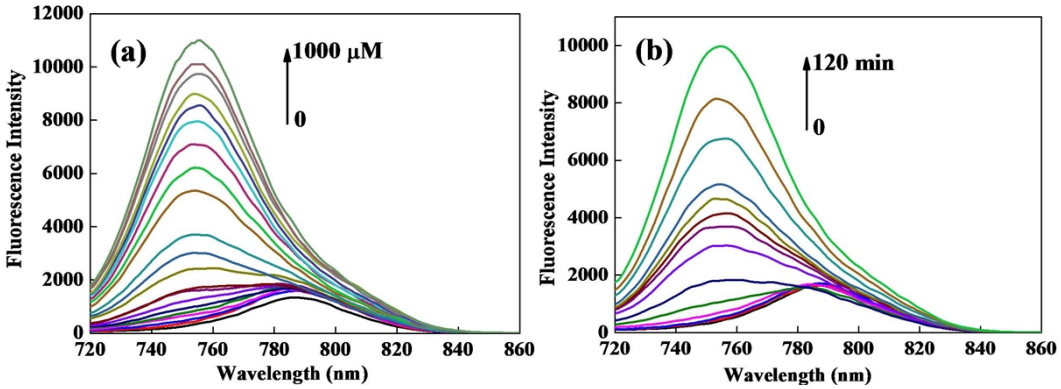

Figure 3 FS variation of Cy-3-NO_2 (10 μM) in the presence of Cys. (a) The FS recorded after Cy-3-NO_2 reacted with 0, 5, 10, 15, 20, 30, 40, 50, 60, 80, 100, 150, 200, 300, 400, 500, 600, 700, 800, 900, and 1000 μMCys for 2h. (b) The FS recorded after Cy-3-NO_2 reacted with Cys (500 μM) for 0, 5, 10, 20, 30, 40, 50, 60, 70, 80, 90, 100, 110, and 120 min. λ_{ex}=710 nm, 50 mM PBS buffer (pH=7.4, 1% CH_3CN), 37 °C.

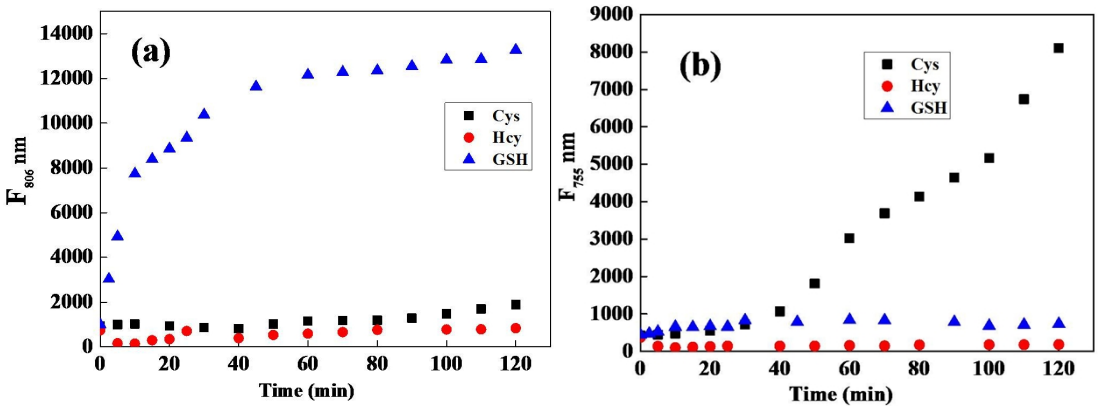

Figure 4 The dependence of FI of Cy-3-NO_2 (10 μM) in the presenceof

biologicalthiols(500μM each) upon reaction times. (a) $\lambda_{ex}/\lambda_{em}$=710/805 nm. (b) $\lambda_{ex}/\lambda_{em}$=710/755 nm. 50 mM PBS buffer (pH=7.4, 1% CH_3CN), 37°C.

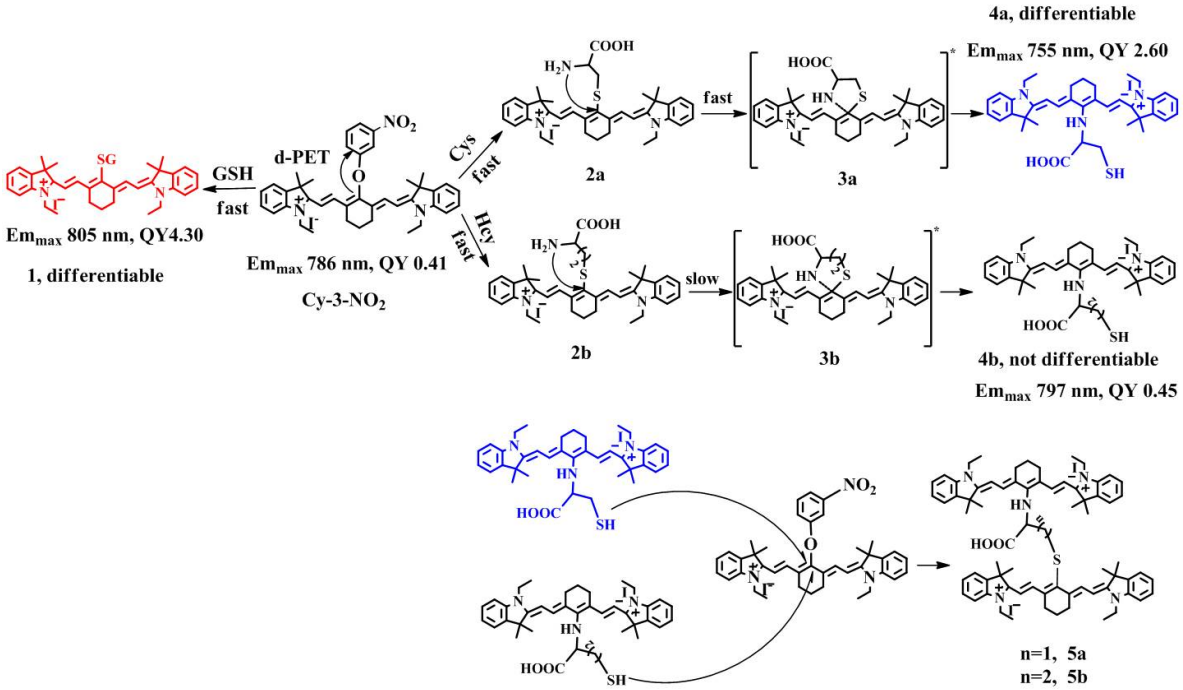

Figure 5 The proposed reaction mechanism of Cy-3-NO_2 towards biothiols.

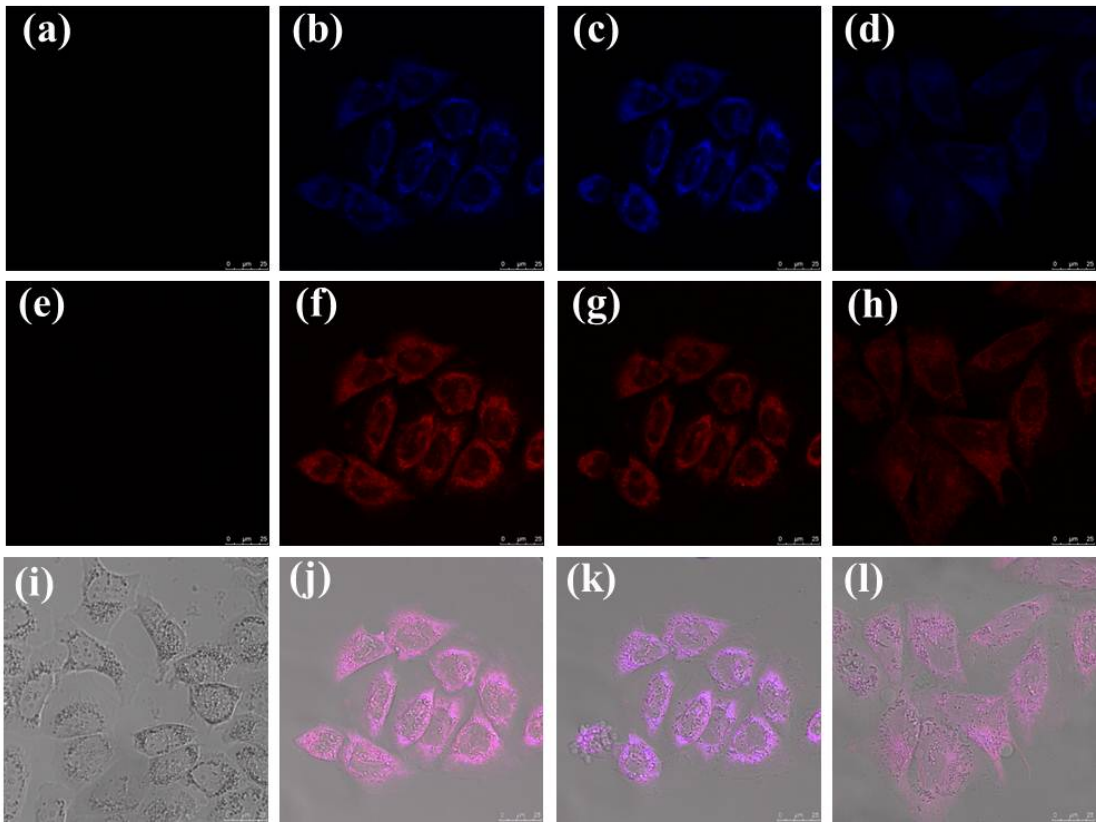

Figure 6 Confocal fluorescence images of GSH and Cys in Hela cells by Cy-3-NO_2.

(a)-(d), images obtained with band path of 700-740 nm (blue fluorescence, pseudo color, assigned to Cys). (e)-(h), images obtained with band path of 760-800 nm (red fluorescence, assigned to GSH). (a), (e), (i), without probe. (b), (f), (j), cells were incubated with 5 μM Cy-3-NO_2 for 15 min. (c), (g), (k), cells were incubated with 5 μM Cy-3-NO_2 for 60 min. (d), (h), (l), the cells were first incubated with NEM for 30 min, then incubated with 5 μM Cy-3-NO_2 for 15 min. 37 ^oC, scale bar = 25 μm, 633 nm laser excitation.

2. Experimental section

General Methods. All chemicals and solvents for synthesis were purchased from commercial suppliers (Sigma-Aldrich, Aladdin) and were used without further purification, unless otherwise stated. The composition of mixed solvents is given by the volume ratio (v/v). All synthesis were carried out under an argon atmosphere. Fluorescence spectra were obtained by a FLS-920 Edinburgh Fluorescence Spectrometer (Edinburgh Instruments Ltd, England) with a Xenon lamp and 1.0-cm quartz cells at the slits of 5.0/5.0 nm. ^{1}H-NMR and ^{13}C-NMR spectra were taken on a Bruker Advance 300-MHz spectrometer (Bruker, Germany), δ values are in ppm relative to TMS. HPLC-HRMS analysis was carried out on a Bruker maxis UHR-TOF Ultra High Resolution Quadrupole-time of flight mass spectrometer (Bruker Co., Ltd., Germany). The fluorescence images of cells were taken using a TCS SP5 confocal laser scanning microscopy (Leica Co., Ltd. Germany) with an objective lens (×20).

Design and Synthesis. Heptamethine cyanine chlorine (Cy.7.Cl) was synthesized in our laboratory.[1] To tune the electrophilic reactivity, selectivity, and sensitivity of the dyes towards biological thiols, different N-, O-, and S-aryl substituents as leaving groups were introduced on the heptamethine cyanine moiety, in which chemical bonds of C-O, C-S, and C-N are acted as the activatable sites for thiols. The oxy-linking NIR dyes were obtained by substituting chlorine atom on Cy.Cl.7 with phenol, m-nitrophenol, p-nitrophenol, and N-(4-hydroxy-3-nitrophenyl)benzamide (NHNB) under alkaline conditions to form Cy-O-Ph, Cy-3-NO_2, Cy-4-NO_2, and Cy-Ph-Ph, respectively. In the case of Cy-2,4-NO_2, 2,4-dinitrofluorobenzene was added to the alkaline solution of ketone cyanine[2] to react for 8 h. The thio-linking NIR dyes were synthesized by substituting chlorine atom on Cy.Cl.7 with thiophenol and p-nitrothiophenol to form Cy-S-Ph and Cy-S-NO_2, respectively. The nitrogen-linking NIR dye of Cy-N-Ph was obtained by the same procedure by using aniline. However, the reaction between nitroaniline and Cy.Cl.7 gave so low productivity that the pure product could not be obtained. We expected that the nitrobenzene derivatives could serve as good quenchers and the number of nitro group or its different substitution position on benzene ring might result in different reactivity towards thiols, resulting in dramatic fluorescence enhancement or spectral shift. The reaction products of Cy-Cys, Cy-Hcy, and Cy-GSH were obtained by incubating Cy-3-NO_2 with excessive amounts of biothiols (Cy-3-NO_2 : biothiols with molar ratio of 1:1000) at room temperature for 24h (a time scale that allowed the intramolecular rearrangement

reaction to complete) and the obtained solutions were applied directly to the test. For the purpose of mechanism investigation, Cy-β-ME was synthesized by nucleophilic substitution on Cy-3-NO_2 by β-mercaptoethanol (β-ME).

Synthesis of Cy-O-Ph.

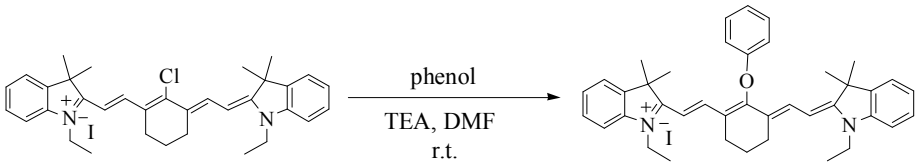

Cy.Cl.7 Cy-O-Ph

Cy.Cl.7 (0.064 g, 0.1 mmol) and phenol (0.188 g, 2.0 mmol) were dissolved in DMF (3 mL), and triethylamine (100 μL) was added. The reaction mixture was stirred under an argon atmosphere for 24 hours at room temperature. Then the solvent was removed under reduced pressure, and the crude product was purified through column chromatography over silica (dichloromethane/methanol = 25/1 as eluent) to give Cy-O-Ph (45 mg, 65%) as green solid. ^{1}H NMR (d6-DMSO, 300 MHz): δ 1.26 (s, 18H), 1.96 (s, 2H), 2.52 (s, 4H), 4.20 (d, 4H, J = 13.8 Hz), 6.20 (d, 2H, J = 14.4 Hz), 7.07 (t, 1H, J = 7.2 Hz), 7.15-7.25 (m, 4H), 7.35-7.45 (m, 6H), 7.53 (d, 2H, J = 7.5 Hz), 7.85 (d, 2H, J = 14.4 Hz). ^{13}C NMR (d6-DMSO, 75 MHz): δ 171.05, 162.38, 159.32, 141.55, 140.98, 140.78, 130.34, 128.48, 124.75, 122.42, 122.30, 121.32, 114.26, 110.95, 99.89, 48.51, 29.04, 27.03, 23.70, 20.67, 12.10. HRMS (ESI$^+$): m/z calcd for [M-I]$^+$ = 569.3526, found 569.3560.

Synthesis of Cy-3-NO_2.

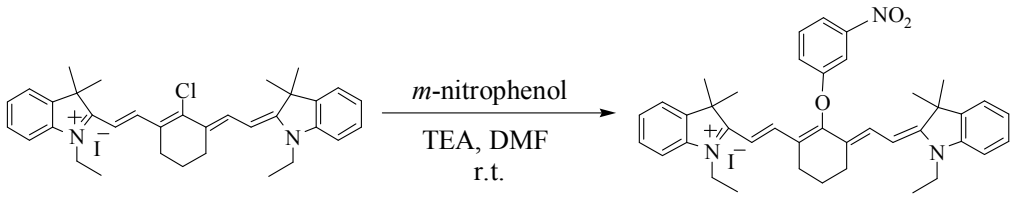

Cy.Cl.7 Cy-3-NO_2

Cy.Cl.7 (0.064 g, 0.1 mmol) and *m*-nitrophenol (0.139 g, 1.0 mmol) were dissolved in DMF (5 mL), and triethylamine (50 μL) was added. The reaction mixture was stirred under an argon atmosphere for 24 hours at room temperature. Then the solvent was removed under reduced pressure, and the crude product was purified through column chromatography over silica (dichloromethane/methanol = 20/1 as eluent) to give Cy-3-NO_2 (47 mg, 63%) as green solid. ^{1}H NMR (d6-DMSO, 300 MHz): δ 1.24-1.28 (m, 18H), 1.91-2.04 (m, 2H), 2.73-2.76 (m, 4H), 4.20 (q, 4H, J = 6.9 Hz), 6.26 (d, 2H, J = 14.4 Hz), 7.19-7.24 (m, 2H), 7.37 (q, 4H, J = 3.9 Hz), 7.53 (d, 2H, J = 7.2 Hz), 7.66-7.69 (d, 2H, J = 9.0 Hz), 7.70-7.77 (m, 2H), 7.96-8.02 (m, 2H). ^{13}C NMR (d6-DMSO, 75 MHz): δ 171.30, 160.77, 159.33, 149.02, 141.51, 141.05, 140.06, 132.06, 128.53, 124.97, 122.45, 121.43, 120.73, 117.39, 111.12, 109.33, 100.37,

48.62, 27.01, 23.69, 20.61, 12.13. HRMS (ESI$^+$): m/z calcd for [M-I]$^+$ =614.3377, found 614.3391.

Synthesis of Cy-4-NO_2.

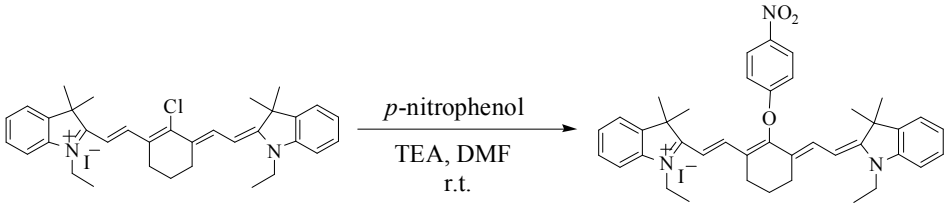

Cy.Cl.7 Cy-4-NO_2

Cy.Cl.7 (0.064 g, 0.1 mmol) and *p*-nitrophenol (0.139 g, 1.0 mmol) were dissolved in DMF (5 mL), and triethylamine (50 μL) was added. The reaction mixture was stirred under an argon atmosphere for 24 hours at room temperature. Then the solvent was removed under reduced pressure, and the crude product was purified through column chromatography over silica (dichloromethane / methanol = 20/1 as eluent) to give Cy-4-NO_2 (44 mg, 60%) as green solid. ^{1}H NMR (d6-DMSO, 300 MHz): δ 1.24-1.28 (m, 18H), 1.92-2.04 (m, 2H), 2.76 (d, 4H, J = 5.4 Hz), 4.19 (q, 4H, J = 6.6 Hz), 6.27 (d, 2H, J = 14.4 Hz), 7.20-7.25 (m, 2H), 7.36-7.42 (m, 4H), 7.47 (d, 2H, J = 9.0 Hz), 7.54 (d, 2H, J = 7.5 Hz), 7.72 (d, 2H, J = 14.1 Hz), 8.37 (d, 2H, J = 9.3 Hz). ^{13}C NMR (d6-DMSO, 75 MHz): δ 171.32, 163.75, 160.58, 142.09, 141.50, 141.05, 139.91, 129.59, 128.54, 126.72, 124.98, 122.45, 120.57, 115.56, 111.15, 100.40, 48.62, 35.07, 31.23, 29.04, 28.99, 28.78, 28.65, 28.53, 27.02, 26.52, 25.07, 23.67, 22.04, 20.52, 12.14. HRMS (ESI$^+$): m/z calcd for [M-I]$^+$ =614.3377, found 614.3411.

Synthesis of Cy-2,4-NO_2.

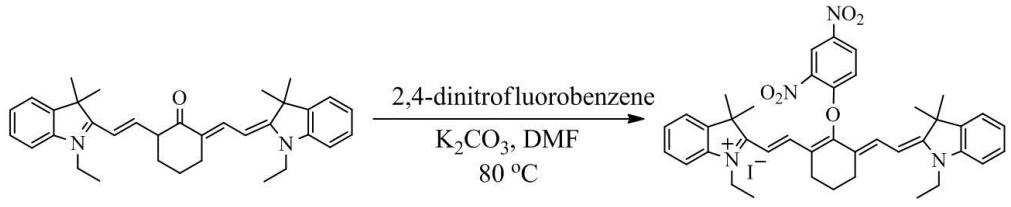

ketone cyanine Cy-2,4-NO_2

Ketone cyanine[2] (0.062 g, 0.1 mmol) and K_2CO_3 (0.069 g, 0.5 mmol) were dissolved in DMF (2 mL), and 2,4-dinitrofluorobenzene (63 μL, 0.5 mmol) was added. The reaction mixture was stirred under an argon atmosphere for 6 hours at 80 ^{o}C. Then the mixture was filtered and the filtrate was concentrated. After that, the crude product was purified through column chromatography over silica (dichloromethane / methanol = 100/3 as eluent) to give Cy-2,4-NO_2 (51 mg, 65%) as green solid. ^{1}H NMR (d6-DMSO, 300 MHz): δ 1.03-1.53 (m, 18H), 1.94 (br, 2H), 2.73 (d, 4H, J = 26.1 Hz), 4.20 (q, 4H, J = 7.2 Hz), 6.26 (d, 2H, J = 14.4 Hz), 7.21-7.26 (m, 2H), 7.37-7.54 (m, 5H), 7.56-7.63 (m, 4H), 8.43 (d, 1H, J = 9.3 Hz), 9.10 (s, 1H). ^{13}C NMR (d6-DMSO, 75 MHz): δ 171.58, 158.37, 154.25, 141.45, 141.29,

141.20, 138.93, 138.34, 129.80, 128.59, 125.23, 122.52, 121.37, 119.91, 116.71, 111.33, 100.93, 55.98, 54.87, 48.76, 40.33, 40.05, 39.78, 39.50, 39.22, 38.94, 38.66, 38.38, 27.01, 26.84, 23.73, 18.52, 12.19. HRMS (ESI^+): m/z calcd for $[M-I]^+$ =659.3228, found 659.3294.

Synthesis of N-(4-hydroxy-3-nitrophenyl)benzamide (NHNB).

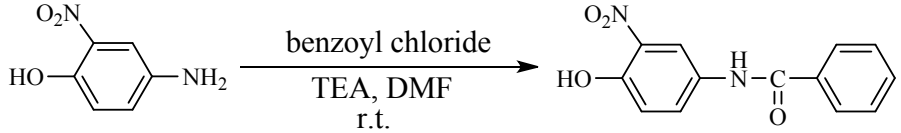

4-amino-2-nitrophenol NHNB

4-amino-2-nitrophenol (0.154 g, 1.0 mmol) was dissolved in DMF (2 mL), and benzoyl chloride (162 μL, 1.4 mmol) in 5 mL dichloromethane was added dropwise at 0 °C. After adding triethylamine (385 μL), the reaction mixture was stirred under an argon atmosphere for 6 hours at room temperature. Then the solvent was removed under reduced pressure, and the crude product was purified through column chromatography over silica (petroleum ether-dichloromethane gradient elution from 1:1 to 1:3) to give N-(4-hydroxy-3-nitrophenyl)benzamide (130 mg, 50%) as orange solid. 1H NMR (d6-DMSO, 300 MHz): δ 7.20 (d, 1H, J = 39 Hz), 7.49-7.66 (m, 4H), 7.94-8.05 (m, 3H), 8.53 (s, 1H), 10.45 (s, 1H). ^{13}C NMR (d6-DMSO, 75 MHz): δ 167.33, 165.46, 148.63, 135.52, 134.43, 132.80, 131.70, 131.05, 130.75, 130.05, 129.25, 128.51, 128.40, 128.16, 127.78, 127.59, 119.33, 116.11. HRMS (ESI^-): m/z calcd for $[M-H]^-$ =257.0556, found 257.0505.

Synthesis of Cy-Ph-Ph.

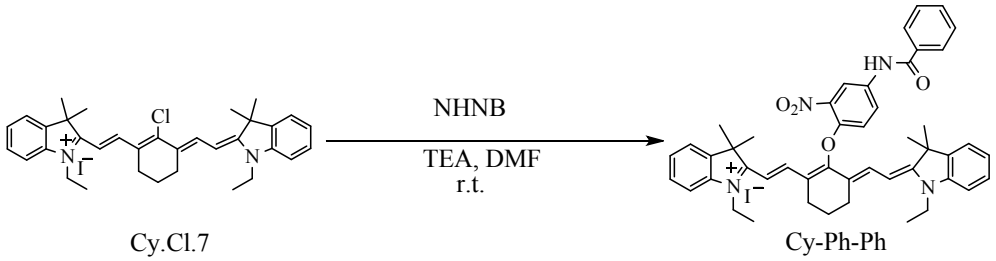

Cy.Cl.7 Cy-Ph-Ph

Cy.Cl.7 (0.032 g, 0.05 mmol) and N-(4-hydroxy-3-nitrophenyl)benzamide (0.258 g, 1.0 mmol) were dissolved in DMF (2 mL), and triethylamine (120 μL) was added. The reaction mixture was stirred under an argon atmosphere for 24 hours at room temperature. Then 50 mL deionized water was added. After the mixture was extracted with dichloromethane (15 mL ×3), the obtained organic phase was dried by anhydrous sodium sulfate and filtered. The filtrate was concentrated and was purified through column chromatography over silica (dichloromethane / methanol = 100/3 as eluent) to give Cy-Ph-Ph (28 mg, 65%) as green solid. ^1H NMR (d6-DMSO, 300 MHz): *δ* 1.12-1.29 (m, 18H), 2.01 (s, 2H), 2.81 (d, 4H, *J* = 24 Hz), 4.20-4.24 (m, 4H), 6.28 (d, 2H, *J* = 14.4 Hz), 7.19-7.24 (m, 3H), 7.36-7.40 (m, 4H), 7.51-7.59 (m, 5H), 7.61-7.78 (m, 2H), 7.90-7.97 (m, 3H), 8.75 (s, 1H), 10.59 (s, 1H). ^{13}C NMR (d6-

DMSO, 75 MHz): δ 171.28, 165.61, 159.98, 146.79, 141.43, 141.04, 139.72, 137.51, 133.91, 133.69, 131.92, 131.41, 129.54, 128.55, 128.39, 127.57, 126.79, 124.94, 122.47, 120.66, 120.12, 115.96, 111.05, 100.37, 64.91, 59.64, 48.59, 29.89, 28.86, 26.93, 23.65, 18.54, 13.98, 13.44, 12.08. LC-HRMS (ESI^+): m/z calcd for $[M-I]^+$ =733.3748, found 733.3833; calcd for $[M-I]^{2+}$=366.6871, found 366.6927.

Synthesis of Cy-S-Ph.

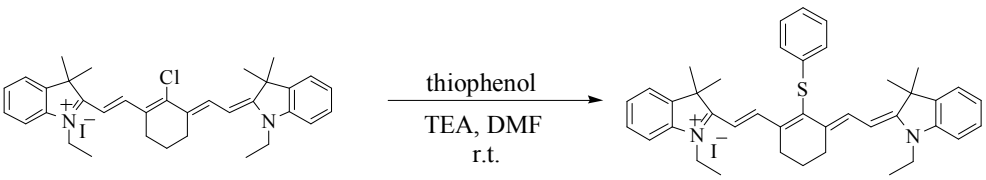

Cy.Cl.7 Cy-S-Ph

Cy.Cl.7 (0.054 g, 0.084 mmol) and thiophenol (0.093 μL, 0.84 mmol) were dissolved in DMF (2 mL), and triethylamine (50 μL) was added. The reaction mixture was stirred under an argon atmosphere for 12 hours at room temperature. Then the solvent was removed under reduced pressure, and the crude product was purified through column chromatography over silica (dichloromethane-methanol gradient elution from 60:1 to 30:1) to give Cy-S-Ph (32 mg, 55%) as yellowgreen solid. ^{1}H NMR (d6-DMSO, 300 MHz): δ 1.26-1.31 (m, 6H), 1.42 (s, 12H), 1.94 (br, 2H), 2.79 (s, 4H), 4.23 (d, 4H, J = 15.0 Hz), 6.33 (d, 2H, J = 14.4 Hz), 7.13 (t, 1H, J = 5.7 Hz), 7.27-7.44 (m, 10H), 7.56 (d, 2H, J = 7.2 Hz), 8.65 (d, 2H, J = 14.1 Hz). ^{13}C NMR (d6-DMSO, 75 MHz): δ 171.50, 148.66, 144.99, 141.58, 141.16, 136.70, 133.12, 129.58, 128.54, 125.68, 125.54, 124.96, 122.44, 111.15, 101.43, 59.72, 48.57, 27.07, 25.84, 20.40, 14.06, 12.20. HRMS (ESI^+): m/z calcd for $[M-I]^+$ =585.3297, found 585.3238.

Synthesis of Cy-S-NO_2.

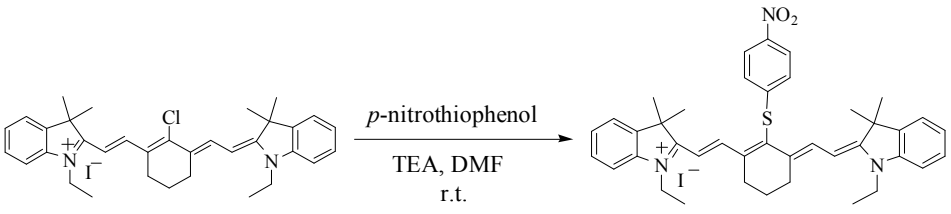

Cy.Cl.7 Cy-S-NO_2

Cy.Cl.7 (0.064 g, 0.1 mmol) and *p*-nitrothiophenol (0.156 g, 1.0 mmol) were dissolved in DMF (3 mL), and triethylamine (50 μL) was added. The reaction mixture was stirred under an argon atmosphere for 12 hours at room temperature, and then was poured into 20 mL diethyl ether to obtain darkgreen precipitate. After filtration, the solid was redissolved by a small amount of dichloromethane and was purified through column chromatography over silica (dichloromethane / methanol = 50/1 as eluent) to give Cy-S-NO_2 (37 mg, 49%) as green solid. ^{1}H NMR (d6-DMSO, 300 MHz): δ 1.18-1.34 (m, 18H), 1.98 (s, 2H), 2.82 (s, 4H), 4.25 (d, 4H, J = 14.1 Hz), 6.36 (d, 2H, J = 14.4 Hz), 7.25 (t, 2H, J = 6.3 Hz), 7.38-7.45 (m, 4H), 7.52-7.56 (m,

4H), 8.20 (d, 2H, J = 9.0 Hz), 8.51 (d, 2H, J = 14.4 Hz). ^{13}C NMR (d6-DMSO, 75 MHz): δ 171.70, 146.66, 145.66, 144.87, 144.18, 141.54, 141.18, 132.96, 128.58, 126.04, 125.14, 124.58, 122.48, 111.31, 101.78, 62.76, 48.81, 45.29, 27.00, 25.86, 12.25, 8.39. HRMS (ESI$^+$): m/z calcd for [M-I]$^+$ =630.3149, found 630.3170.

Synthesis of Cy-N-Ph.

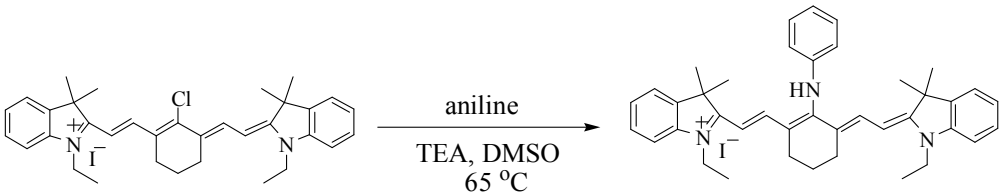

Cy.Cl.7 Cy-N-Ph

Cy.Cl.7 (0.037 g, 0.058 mmol) and aniline (56.6 μL, 0.58 mmol) were dissolved in DMSO (3 mL), and triethylamine (50 μL) was added. The reaction mixture was stirred under an argon atmosphere for 12 hours at 65 °C. Then 50 mL deionized water was added and the mixture was extracted with ethyl acetate (15 mL ×3). The obtained organic phase was dried by anhydrous sodium sulfate and filtered. The filtrate was concentrated and was purified through column chromatography over silica (dichloromethane-methanol gradient elution from 100:1 to 50:1) to give Cy-N-Ph (27 mg, 67%) as blue-green solid. ^{1}H NMR (d6-DMSO, 300 MHz): δ 1.19-1.24 (m, 6H), 1.56 (s, 12H), 1.76 (t, 2H, J = 6.6 Hz), 2.00 (q, 2H, J = 4.5 Hz), 3.52 (s, 6H), 3.97 (t, 4H, J = 4.5 Hz), 5.32 (t, 1H, J = 4.5 Hz), 5.74 (d, 2H, J = 12.9 Hz), 7.02-7.13 (m, 4H), 7.27-7.35 (m, 4H), 7.45 (d, 2H, J = 7.2 Hz). HRMS (ESI$^+$): m/z calcd for [M-I]$^+$ =568.3686, found 568.3681.

Synthesis of Cy-β-ME.

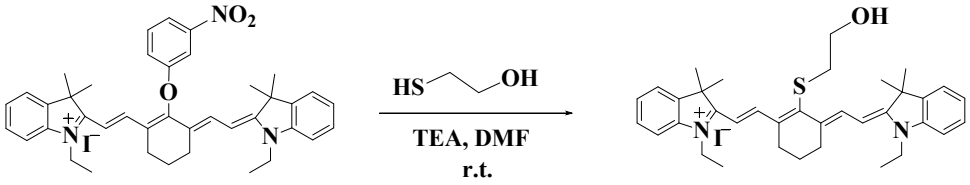

Cy-3-NO_2 (74 mg, 0.1 mmol) was dissolved in DMF (5 mL), and β-ME (74 μL, 1 mmol) and triethylamine (50 μL) were added. The reaction mixture was stirred under an argon atmosphere for 24 hours at room temperature. Then the solvent was removed under reduced pressure, and the crude product was purified through column chromatography over silica (dichloromethane/ethanol = 20/1 as eluent) to give Cy-β-ME (26.0 mg, 38%) as green solid. ^{1}H NMR (d6-DMSO, 300 MHz): δ 1.70 (s, 12H), 1.84 (t, 2H, J = 5.4 Hz), 2.01 (q, 2H, J = 3.7 Hz), 2.68 (t, 4H, J = 6.0 Hz), 2.90 (t, 2H, J = 6.6 Hz), 3.55 (t, 6H, J = 6.5 Hz), 4.27 (q, 4H, J = 6.5 Hz), 6.33 (d, 2H, J = 14.1 Hz), 7.24-7.30 (m, 2H), 7.40-7.43(m, 4H), 7.69 (d, 2H, J = 7.5 Hz), 8.82(d, 2H, J = 14.1 Hz). ^{13}C NMR (d6-DMSO, 75 MHz): δ 171.77, 145.49, 142.13, 141.42, 139.44, 133.14, 128.93, 125.16, 122.88, 111.33, 101.25, 72.62, 60.50, 56.37, 49.18, 31.61,

29.32, 27.65, 26.04, 22.43, 20.96, 18.90, 14.28, 12.49. HRMS (ESI^+): m/z calcd for $[M-I]^+$ =553.3247, found 553.3205.

Fluorescence Spectral Measurement. A stock solution (1 mM) of the probe in CH_3CN was prepared. During the measurement, a sample solution was prepared by mixing an appropriate amount of the stock solution of the probe with an appropriate amount of each biothiol and finally diluting with PBS buffer (50 mM, pH 7.4) to obtain the desired concentration. The fluorescence intensities of the NIR dyes were similarly measured with a slit width of 5 nm × 5 nm. The detection was performed at 37 ^oC.

Quantum Yield Measurement. Fluorescence quantum yields for the synthesized dyes were determined by using ICG (Φ_f = 0.13 in 0.1 M PBS of pH 7.40) as a fluorescence standard.[3] The quantum yield was calculated using the following equation:

$$\Phi_{F(X)} = \Phi_{F(S)} (A_S F_X / A_X F_S) (n_X / n_S)^2$$

Where Φ_F is the fluorescence quantum yield, A is the absorbance at the excitation wavelength, F is the area under the corrected emission curve, and n is the refractive index of the solvents used. Subscripts $_S$ and $_X$ refer to the standard and to the unknown, respectively. For the synthesized dyes, the excitation wavelength was at 700 nm while keeping the absorption below 0.05.

Cell Confocal Imaging Experiment. Hela cells were maintained following protocols provided by the American Type Tissue Culture Collection. Cells were seeded at a density of 1 × 10^6 cells mL^{-1} in Dulbecco's Modified Eagle Medium (DMEM) supplemented with 10% fetal bovine serum (FBS) and 1% antibiotics (penicillin /streptomycin, 100 U mL^{-1}). Cultures were maintained in a humidified incubator at 37 °C, in 5% CO_2/95% air. Cells were passed and plated on 18-mm glass coverslips in culture dish. A solution of 5 μM probe in culture solution was prepared before confocal imaging. Excitation of probe-loaded cells at 633 nm was carried out with a HeNe laser and the emission was collected between 700-800 nm for Cy-Ph-Ph, and 700-740/760-800 nm for Cy-3-NO_2. Prior to imaging, the medium was removed. Cell imaging was carried out after washing cells with PBS buffer (pH 7.4, 0.10 M) for three times.

Colocalization Imaging Experiments in Hela Cells. Hela cells were passed and dispersed on 24 mm glass coverslips at 37 °C, 5% CO_2 1 day before imaging. Then cells were incubated with Mito-Tracker Green (50 nM) and Cy-3-NO_2 (5 μM) for 15 min. The medium was removed and cells were washed with PBS (10 mM, pH 7.4) for three times. Confocal images of cells fluorescence of the Mito-Tracker Green were captured using a 488 nm laser, the collection window is 495–520 nm. The excitation wavelength of Cy-3-NO_2 is 633 nm, and the collection window is 700–800 nm.

HPLC-HRMS Experiment. Chromatographic separation by HPLC (DIONEX Ultimate 3000) was performed with a C18 column (250 mm × 4.6 mm i.d., 5 μm, DIONEXC18) using a mobile phase composed of 1‰ HCOOH and methanol with differing proportions. The flow rate is 0.3 mL/min and the detection wavelength is 670 nm. The HPLC system was interfaced to the ESI-MS system (maxis UHR-TOF

Ultra High Resolution Quadrupole-time of flight mass spectrometer, Bruker Co., Ltd., Germany). Sample of 8.0 μL were injected into the column using an autosampler.

3. Molecular structure of biothiols and sulfydryl-containing control compounds

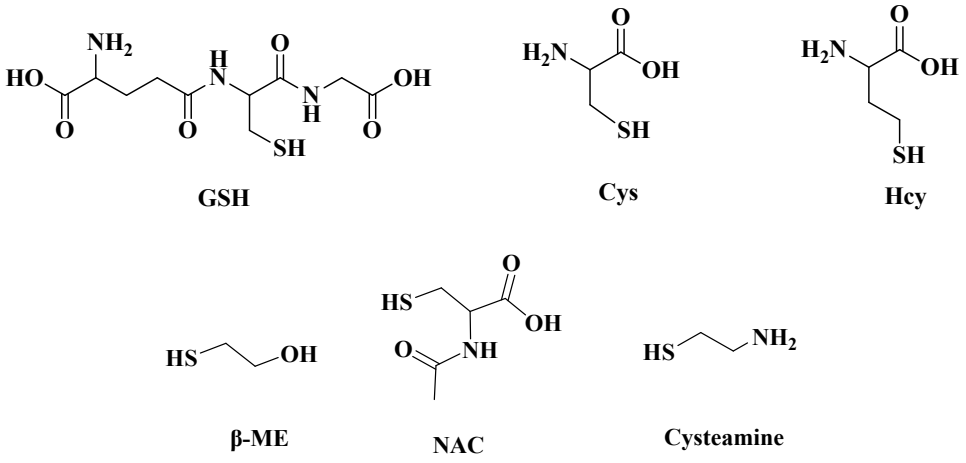

Scheme S1. The molecular structure of biothiols and sulfydryl-containing control compounds.

4. DFT calculation results[4]

Table S1. Bond length, bond order, and net charge of central carbon obtained from DFT calculations.

Dyes	Bond length$_{C-X}$/Å	Bond order$_{C-X}$	Net charge of central carbon
Cy-O-Ph	1.386 (C-O)	0.9372 (C-O)	0.381
Cy-3-NO_2	1.392 (C-O)	0.9230 (C-O)	0.368
Cy-4-NO_2	1.394 (C-O)	0.9190 (C-O)	0.366
Cy-2,4-NO_2	1.402 (C-O)	0.8980 (C-O)	0.353
Cy-Ph-Ph	1.394 (C-O)	0.9146 (C-O)	0.371
Cy-S-Ph	1.810 (C-S)	1.0304 (C-S)	-0.122
Cy-S-NO_2	1.814 (C-S)	1.0194 (C-S)	-0.132
Cy-N-Ph	1.394 (C-N)	1.1139 (C-N)	0.244

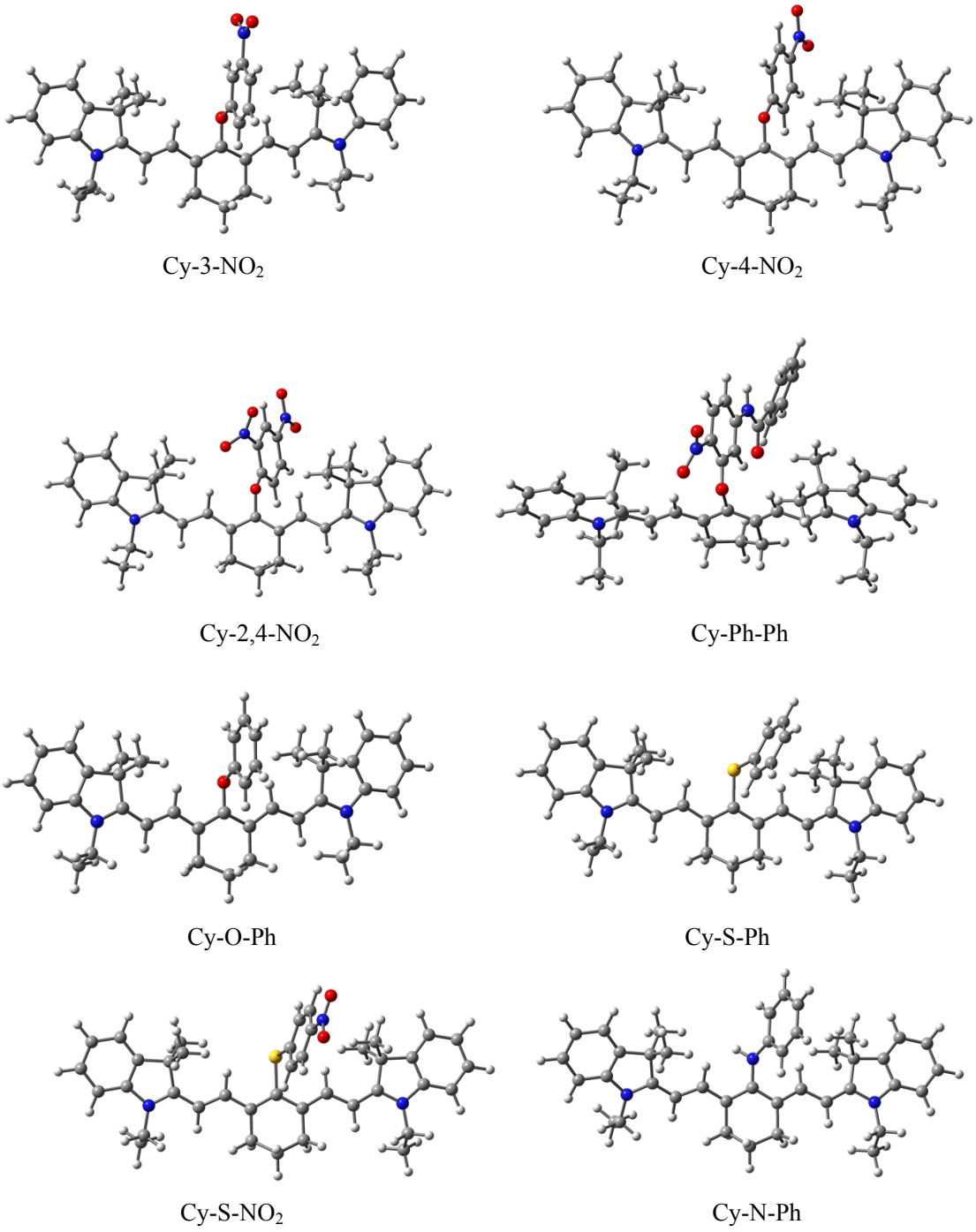

Figure S1. The optimized molecular structure of the synthesized NIR dyes from DFT calculation.

5. The summarized photophysical properties of the dyes after reaction with biological thiols

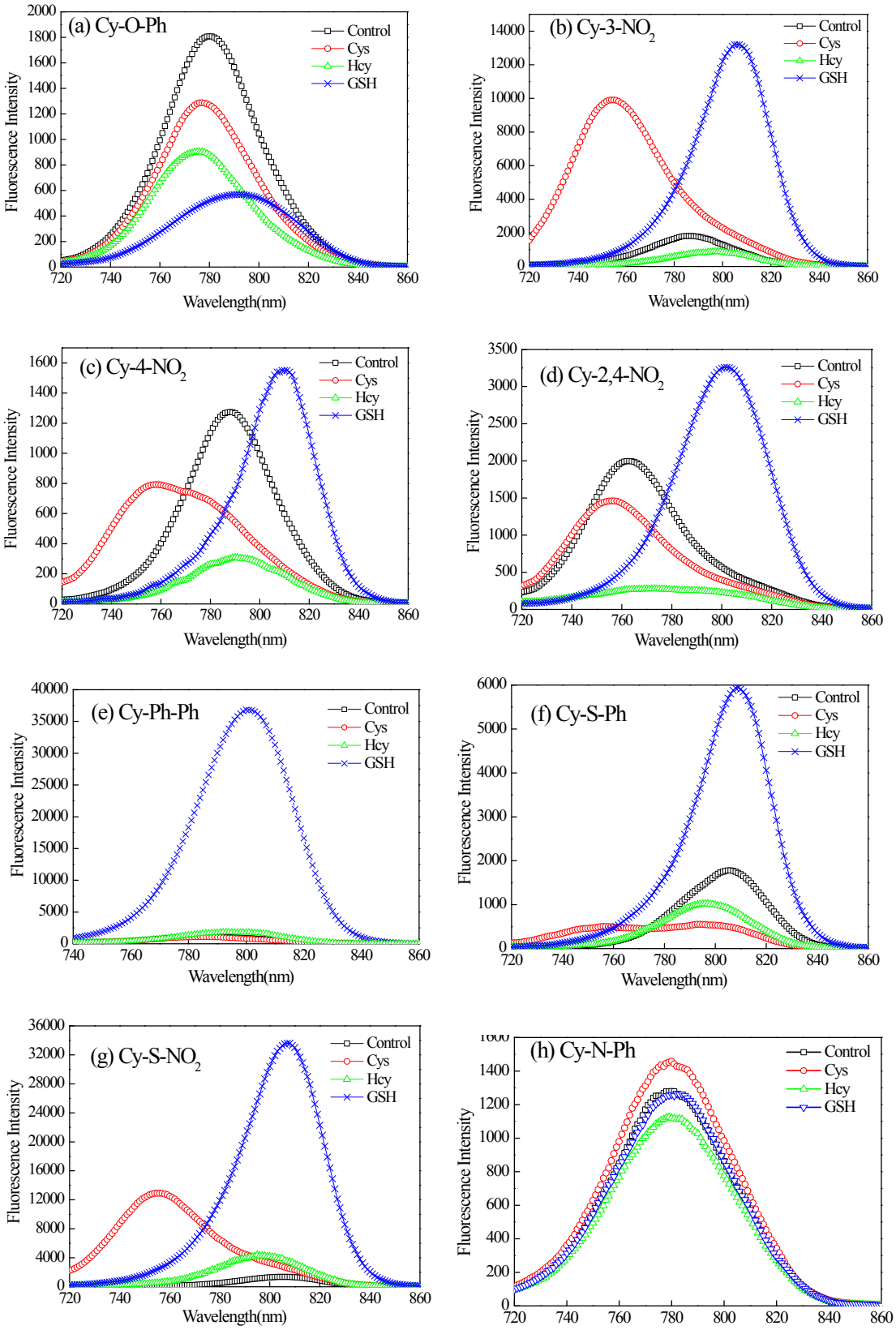

Figure S2. Fluorescence emission spectra (λex=710 nm) of the synthesized NIR dyes (10 μM) after reaction with 500 μM of GSH, Cys, and Hcy respectively in 50 mM PBS buffer (pH=7.4, 1% CH_3CN) at 37 °C for 2h. (a) Cy-O-Ph, (b) Cy-3-NO_2, (c) Cy-4-NO_2, (d) Cy-2,4-NO_2, (e) Cy-Ph-Ph, (f) Cy-S-Ph, (g) Cy-S-NO_2, (h) Cy-N-Ph.

Table S2. The photophysical properties of the dyes after reaction with biological thiols. The experimental conditions can be found in the caption of Figure S2.

Dyes (λem, nm)	Dye+Cys			Dye+Hcy			Dye+GSH		
	New peak or not (λem, nm)	red/blue shift (△λ, nm)	F/F_0	New peak or not (λem, nm)	red/blue shift (△λ, nm)	F/F_0	New peak or not (λem, nm)	red/blue shift (△λ, nm)	F/F_0
Cy-O-Ph (780 nm)	yes (778 nm)	blue shift (2 nm)	0.71	yes (776 nm)	blue shift (4 nm)	0.49	yes (795 nm)	red shift (15 nm)	0.31
Cy-3-NO_2 (786 nm)	yes (755 nm)	blue shift (33 nm)	5.5	yes (797 nm)	red shift (11 nm)	0.49	yes (805 nm)	red shift (20 nm)	7.3
Cy-4-NO_2 (788 nm)	yes (758 nm)	blue shift (30 nm)	0.59	no	—	0.24	yes (808 nm)	red shift (20 nm)	1.2
Cy-2,4-NO_2 (760 nm)	yes (755 nm)	blue shift (5 nm)	0.73	no	—	0.14	yes (802 nm)	red shift (42 nm)	1.6
Cy-Ph-Ph (783 nm)	no	—	0.89	yes (797 nm)	red shift (14 nm)	1.5	yes (803 nm)	red shift (20 nm)	43.1
Cy-S-Ph (805 nm)	yes (755 nm)	blue shift (50 nm)	0.31	yes (797 nm)	blue shift (8 nm)	0.57	no	—	3.3
Cy-S-NO_2 (806 nm)	yes (755 nm)	blue shift (51 nm)	9.8	yes (797 nm)	blue shift (9 nm)	3.3	yes (808 nm)	red shift (2 nm)	25.4
Cy-N-Ph (780 nm)	no	—	1.20	no	—	0.92	no	—	0.98

6. The fluorescence spectra of Cy-3-NO_2 in the presence of biothiols

A good linearity between the FI and the GSH concentration in the range of 0.25-40 μM was obtained (Figure S3b). As to Cys, a good linearity between the FI and the Cys concentration in the range of 5.0-100 μM was observed (Figure S4b).

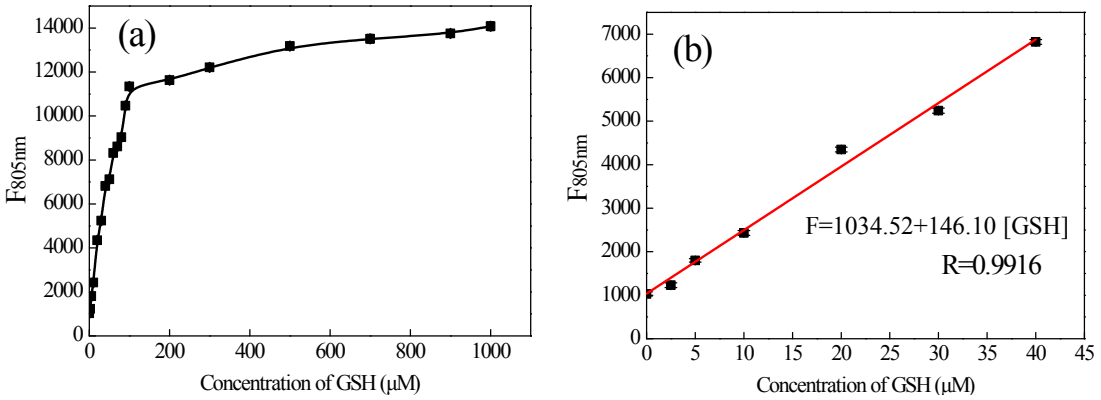

Figure S3. Dependence of FI of Cy-3-NO_2 (10 μM) upon different GSH concentrations. (a) FI of Cy-3-NO_2 with 0, 2.5, 5, 10, 20, 30, 40, 50, 60, 70, 80, 90, 100, 200, 300, 400, 500, 700, 900, and 1000 GSH. (b) The linear relationship between FI of Cy-3-NO_2 and GSH concentrations. Experimental conditions: 50 mM PBS buffer (pH=7.4, 1% CH_3CN), 37 °C incubation for 2h, $\lambda_{ex}/\lambda_{ex}$=710/805 nm.

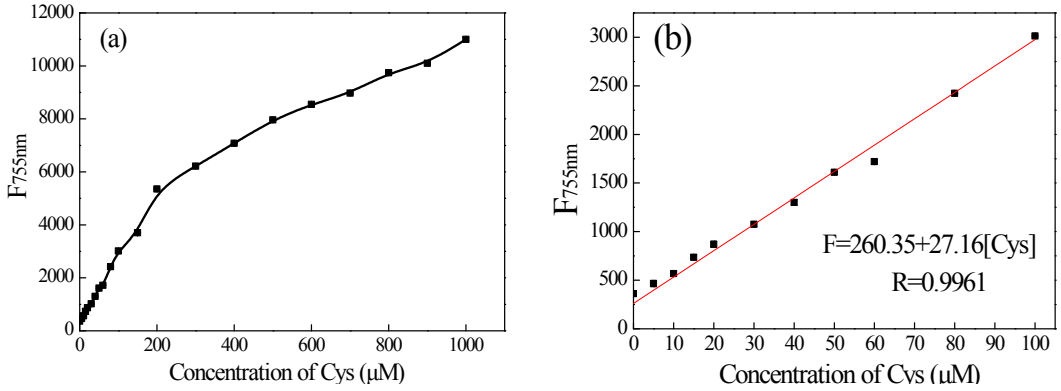

Figure S4. Dependence of FI of Cy-3-NO_2 (10 μM) upon different Cys concentrations. (a) FI of Cy-3-NO_2 with 0, 5, 10, 15, 20, 30, 40, 50, 60, 80, 100, 150, 200, 300, 400, 500, 600, 700, 800, 900, and 1000 μM Cys. (b) The linear relationship between FI of Cy-3-NO_2 and Cys concentrations. Experimental conditions: 50 mM PBS buffer (pH=7.4, 1% CH_3CN), 37 °C incubation for 2h, $\lambda_{ex}/\lambda_{ex}$=710/755 nm.

The FS of Cy-3-NO_2 remained almost unchanged in the Hcy concentration range of 0~60 μM (Figure S5a). Subsequently, the FI decreased with increasing Hcy concentration, and the Em_{max} red-shifted to 797 nm (Figure S5b). The dynamic investigation showed a rapid falling of the FI to the lowest level within the first 10 min (Figure S6a), and then the FI slowly increased with increasing incubation time, accompanied by a red shift of Em_{max} to 797 nm. Even though after 2h, the FI was still lower than the control (Figure S6b).

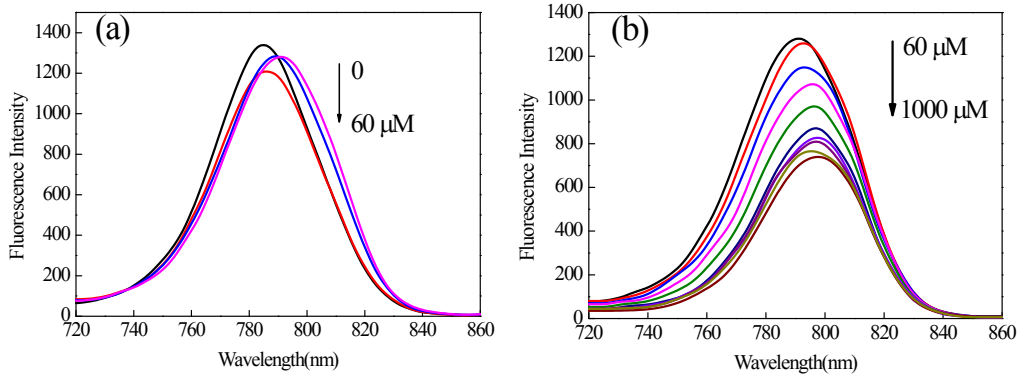

Figure S5. FS variation of Cy-3-NO_2 (10 μM) in the presence of different concentrations of Hcy. (a) 0, 10, 40, and 60 μM Cys. (b) 60, 70, 100, 200, 300, 400, 500, 600, 900, and 1000 μM Hcy. Experimental conditions: λ_{ex}=710 nm, 50 mM PBS buffer (pH=7.4, 1% CH_3CN), 37 °C incubation for 2h.

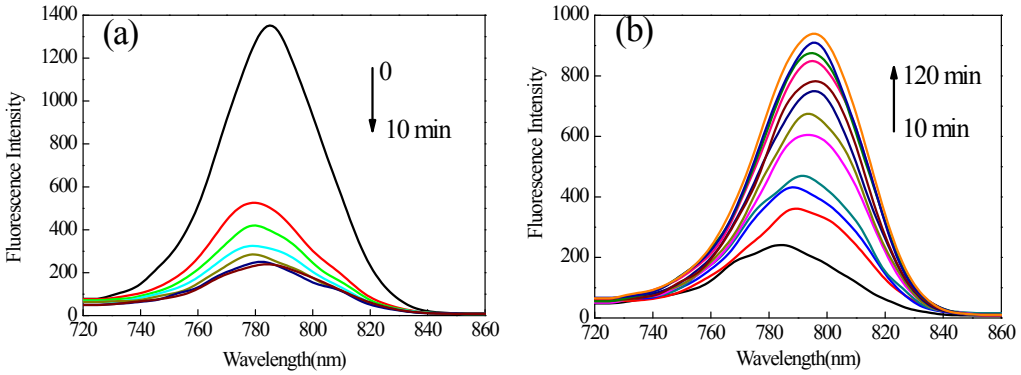

Figure S6. The FS recorded after Cy-3-NO_2 (10 μM) reacted with Hcy (500 μM) for (a) 0, 1, 2, 4, 6, 8, and 10 min and (b) 10, 15, 20, 25, 40, 50, 60, 70, 80, 100, 110, and 120 min. Experimental conditions: λ_{ex}=710 nm, 50 mM PBS buffer (pH=7.4, 1% CH_3CN), 37 °C.

7. Effect of pH on sensing behavior of Cy-3-NO_2

The investigation on pH (Figure S7) showed that the Cy-3-NO_2 is stable enough in a relatively wide pH range of 6.5-9.0, and displays the obvious response for GSH and Cys simultaneously at pH 7.4.

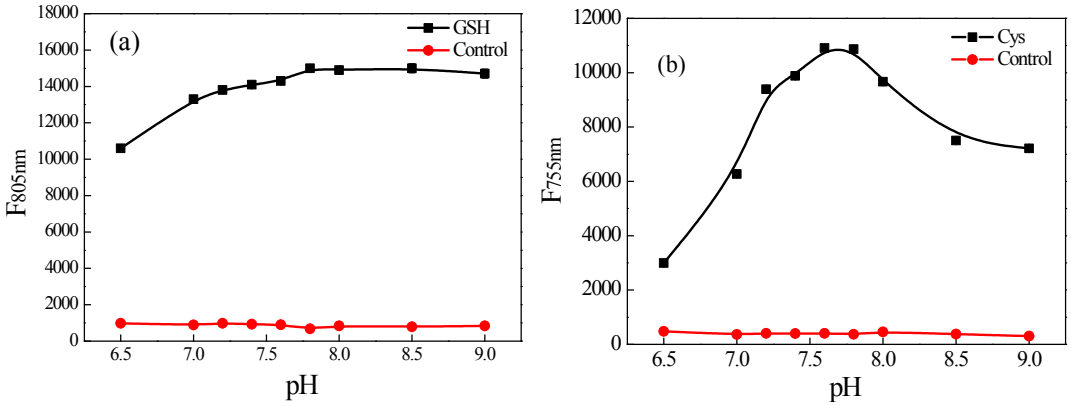

Figure S7. Effect of pH on the reaction of (a) Cy-3-NO_2 and GSH ($\lambda_{ex/em}$=710/805 nm) and (b) Cy-3-NO_2 and Cys ($\lambda_{ex/em}$=710/755 nm). The concentrations of Cy-3-NO_2 and tested biothiols were 10 μM and 500 μM, respectively. 50 mM PBS buffer (pH=7.4, 1% CH_3CN), 37 °C incubation for 2h.

8. Selectivity investigation of Cy-3-NO_2

To evaluate the specific response of Cy-3-NO_2 to GSH and Cys simultaneously, various species were examined in parallel under the same conditions, including amino acids, glucose, GSSG, ascorbic acid, H_2O_2, NO, and NO_2^- (Figure S8). It can be seen that the fluorescence of Cy-3-NO_2 apparently enhanced upon reaction with GSH or Cys in the respective detection channel. While the fluorescence variations induced by

other bio-substances was neglectable. These results suggest that Cy-3-NO_2 is highly selective for the targeting biothiols.

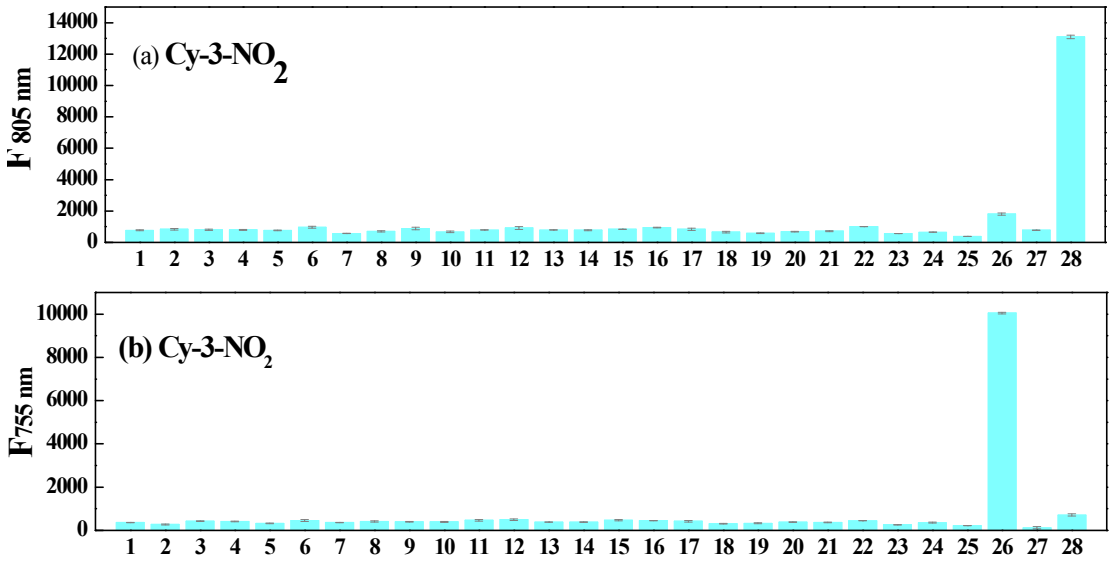

Figure S8. Fluorescence intensity changes of (a) Cy-3-NO_2 (10 μM, $\lambda_{ex/em}$=710/805 nm) and (b) Cy-3-NO_2 (10 μM, $\lambda_{ex/em}$=710/755 nm) upon addition of various amino acids and biologically related substances after 2h in 50 mM PBS buffer (pH=7.4, 1% CH_3CN) at 37 °C. (1) probe only, (2) Gly, (3) Ala, (4) Arg, (5) Asn, (6) Asp, (7) Gln, (8) Glu, (9) His, (10) Val, (11) Leu, (12) Lys, (13) Met, (14) Pro, (15) Ser, (16) Thr, (17) Trp, (18) Tyr, (19) Ile, (20) Glucose (500 μM), (21) Ascorbic acid (500 μM), (22) GSSG (500 μM), (23) NO (250 μM), (24) NO_2^- (500 μM), (25) H_2O_2 (500 μM), (26) Cys (500 μM), (27) Hcy (500 μM), (28) GSH (500 μM). The concentrations of the tested amino acids were all 500 μM.

9. Fluorescence spectra of Cy-3-NO_2 in the presence of sulfydryl-containing control compounds

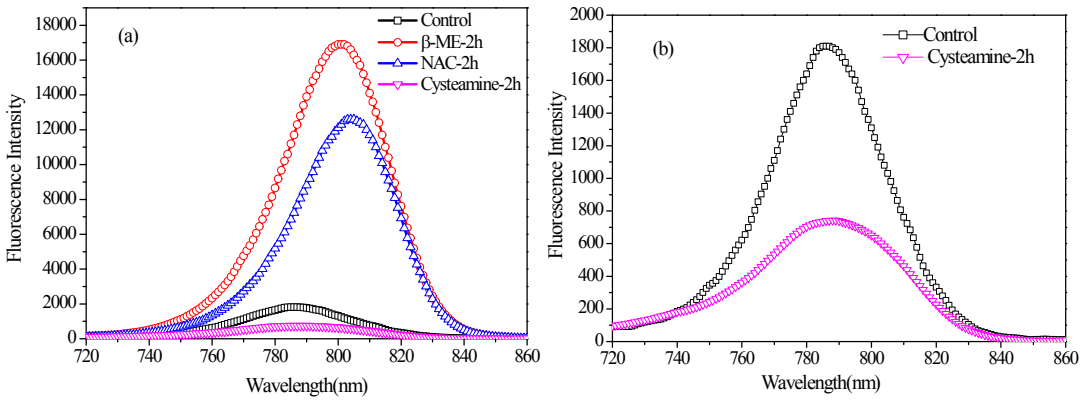

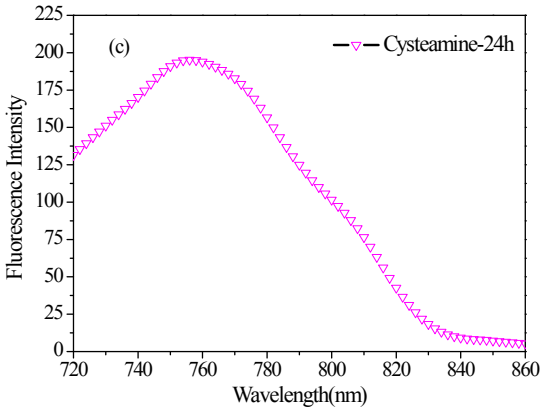

Figure S9. The FS recorded after Cy-3-NO_2 (10 μM) reacted with 500 μM β-ME, NAC, and cysteamine. (a) The overall FS after reaction for 2h. (b) The enlarged FS of the control and Cy-3-NO_2+cysteamine after 2h. (c) The FS of Cy-3-NO_2+cysteamine after 24h. Experimental conditions: λ_{ex}=710 nm, 50 mM PBS buffer (pH=7.4, 1% CH_3CN), 37 ^oC.

10. ^{1}HNMR spectra investigation on Cy-3-NO_2 in the presence of β-ME

We performed ^{1}H NMR spectral analysis of Cy-3-NO_2 in the presence of β-ME (Figure S10). In the presence of 1.5 equiv β-ME, the vinylic protons of Cy-3-NO_2 were markedly shifted to downfield regions. The shift of H^a at 7.98 ppm gradually disappeared and a new shift at 8.82 ppm emerged, while the shift of H^b at 6.26 ppm gradually disappeared with a new emerged shift at 6.33 ppm. In the same time, the proton of *o*-position in the nitrophenol was shifted to an upfield region (H^c 7.70 to 7.58 ppm) owing to the release of free *m*-nitrophenol. For confirmation, the spectrum of an authentic Cy-β-ME (Figure S10G) was listed and high coincidence can be found between the product (Figure S10F) and Cy-β-ME. The NMR spectral variations suggested that the nitrophenol of Cy-3-NO_2 was readily substituted with a thiol group, which is accordance with the fluorescence changes (Figure S10).

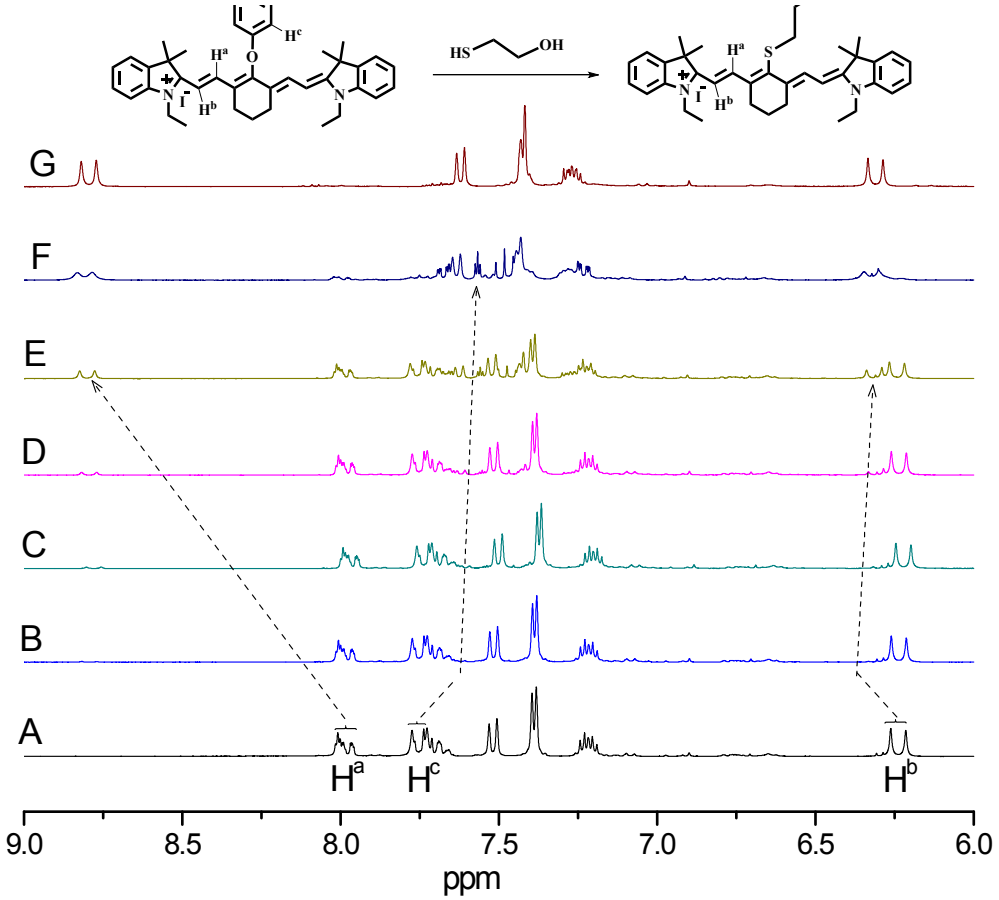

Figure S10. Partial ^{1}H NMR spectra of Cy-3-NO_2 (15 mg) in the presence of β-ME (1.5 equiv) in d6-DMSO. (A) Cy-3-NO_2, (B) 0.5 h after addition of ME, (C) 1 h, (D) 2 h, (E) 6 h, (F) 24 h, (G) Cy-β-ME.

11. MS spectra of Cy-3-NO_2 in the presence of sulfydryl-containing control compounds

More detailed information can be obtained from HRMS. In the presence of β-ME or NAC, the peaks assigned to the thiol-substituted products of **6**/**7** (the numbered compound can be found in the proposed reaction mechanism in Figure S12) were found, respectively (Figure S11a and S11b). However, in the case of cysteamine, a bridging product of $(Cy)_2$-cysteamine (**10**) besides the thiol/amino substituted product (**8**/**9**) was observed (Figure S11c and S11d), indicating an intermolecular nucleophilic substitution in the presence of thiol containing amino acids (Table S3). Therefore, based on the FS spectra, NMR spectra, and HRMS spectra, the proposed reaction mechanism of Cy-3-NO_2 upon control compounds addition was shown in Figure S12, exhibiting the intramolecular rearrangement cascade reaction and the subsequent intermolecular nucleophilic coupling reactions.

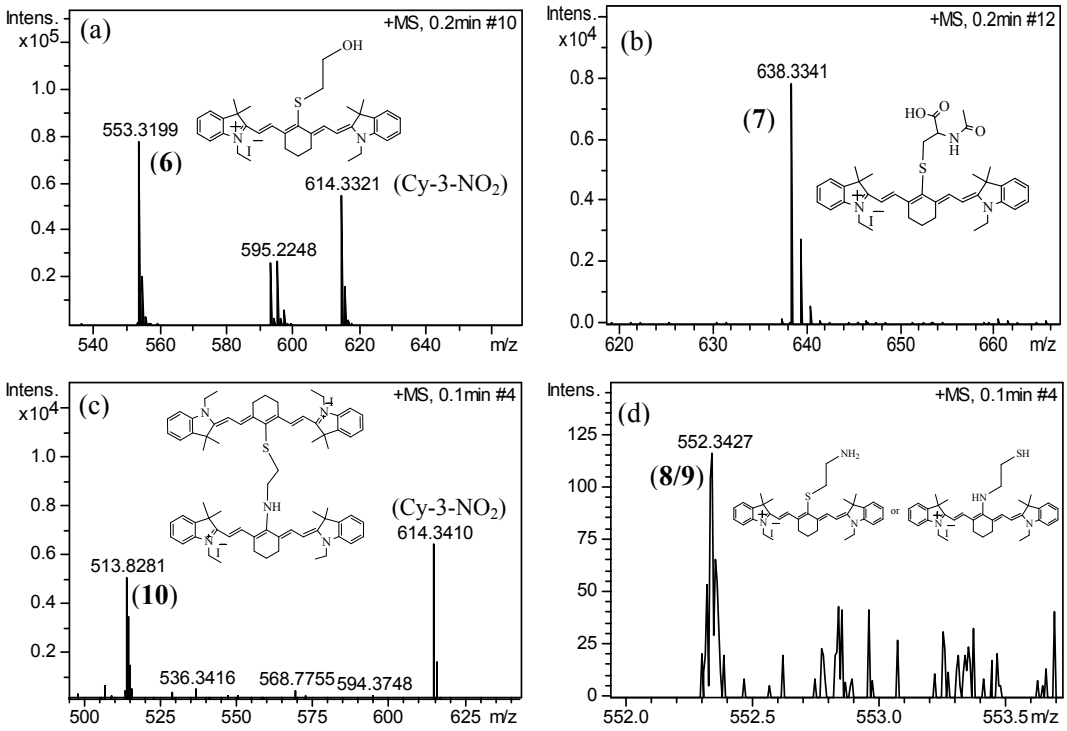

Figure S11. Mass spectra recorded after Cy-3-NO_2 (10 μM) incubated with sulfydryl-containing control compounds (500 μM) in a 50 mM PBS buffer (pH=7.4) at 37 °C. (a) β-ME, 2h incubation; (b) NAC, 2h incubaiton; (c) and (d) cysteamine, 24h incubation.

Table S3. The molecular formula and *m*/*z* of compounds in Figure S11.

Compounds	molecular formula	*m*/*z* obsd	*m*/*z* cald
6	$C_{36}H_{45}IN_2OS$	$[M-I]^+$ 553.3199	$[M-I]^+$ 553.3247
7	$C_{39}H_{48}IN_3O_3S$	$[M-I]^+$ 638.3342	$[M-I]^+$ 638.3410
8/**9**	$C_{36}H_{46}IN_3S$	$[M-I]^+$ 552.3427	$[M-I]^+$ 552.3407
10	$C_{70}H_{85}I_2N_5S$	$[M-2I]^{2+}$ 513.8281	$[M-2I]^{2+}$ 513.8257

12. Reaction mechanism of Cy-3-NO_2 towards sulfydryl-containing control compounds

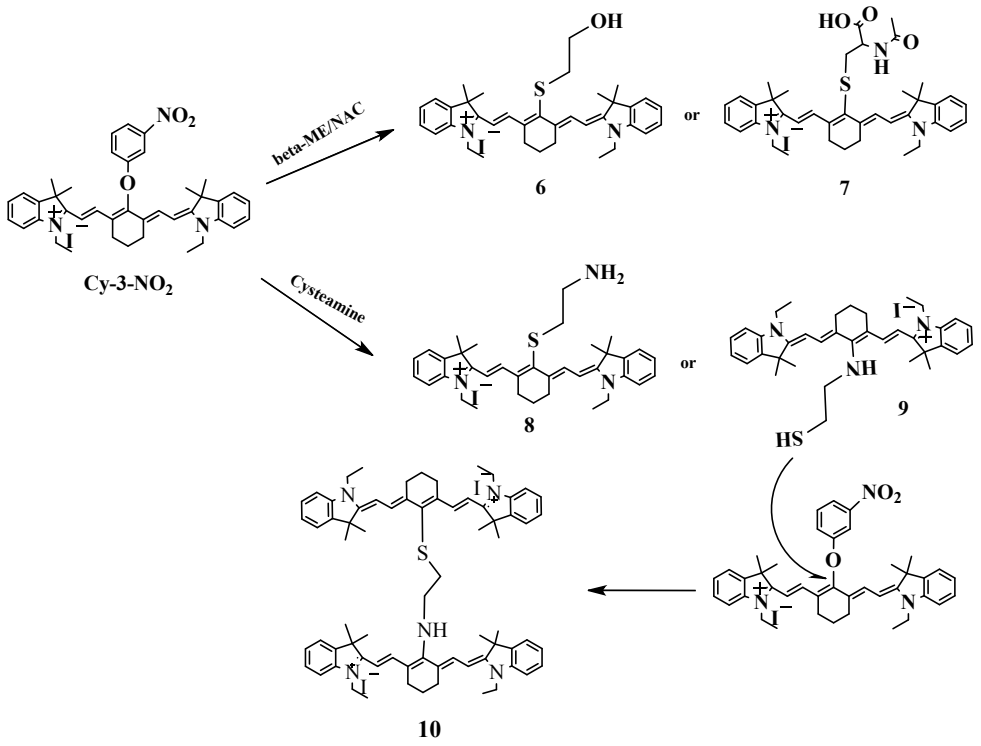

Figure S12. The proposed mechanism of Cy-3-NO_2 in the presence of sulfydryl-containing control compounds.

13. MS spectra of Cy-3-NO_2 in the presence of biothiols

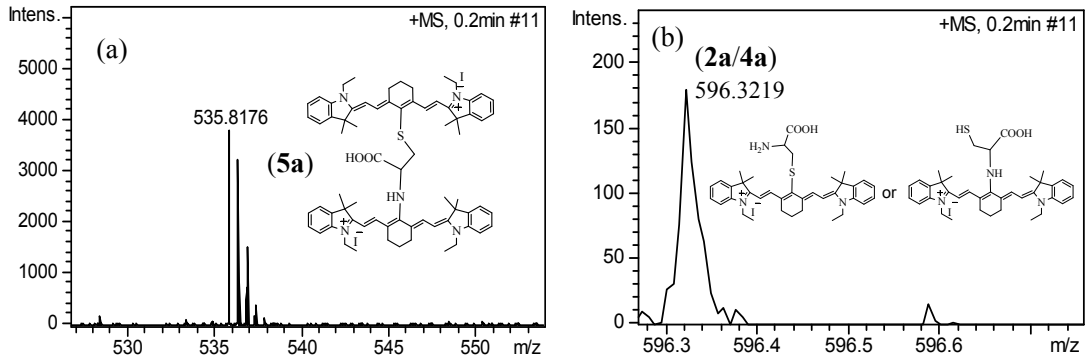

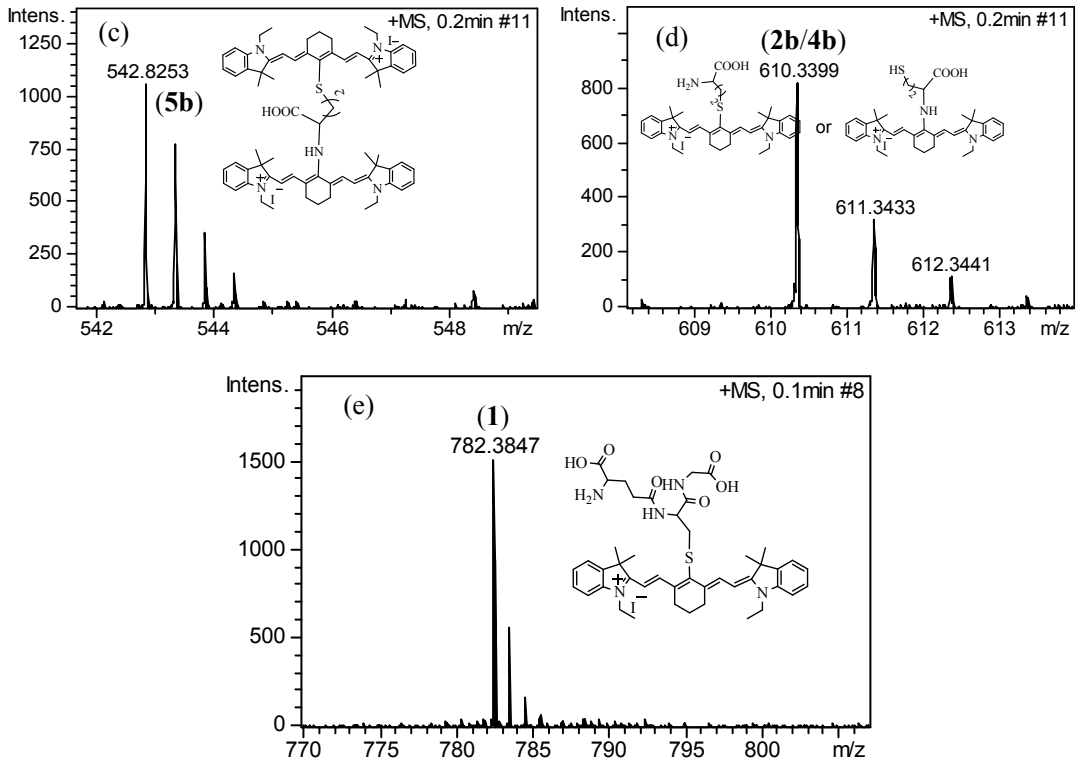

Figure S13. Mass spectra recorded after Cy-3-NO_2 (10 μM) incubated with (a) and (b) 500 μM Cys; (c) and (d) 500 μM Hcy; (e) 500 μM GSH in a 50 mM PBS buffer (pH=7.4) at 37 ^oC for 2h.

Table S4. The molecular formula and *m*/*z* of compounds in Figure S13.

Compounds	molecular formula	*m*/*z* obsd	*m*/*z* cald
5a	$C_{71}H_{85}I_2N_5O_2S$	$[M-2I]^{2+}$ 535.8176	$[M-2I]^{2+}$ 535.8207
2a/**4a**	$C_{37}H_{46}IN_3O_2S$	$[M-I]^{+}$ 596.3219	$[M-I]^{+}$ 596.3305
5b	$C_{72}H_{87}I_2N_5O_2S$	$[M-2I]^{2+}$ 542.8253	$[M-2I]^{2+}$ 542.8284
2b/**4b**	$C_{38}H_{48}IN_3O_2S$	$[M-I]^{+}$ 610.3399	$[M-I]^{+}$ 610.3462
1	$C_{44}H_{56}IN_5O_6S$	$[M-I]^{+}$ 782.3847	$[M-I]^{+}$ 782.3946

14. The proposed overall reaction mechanism

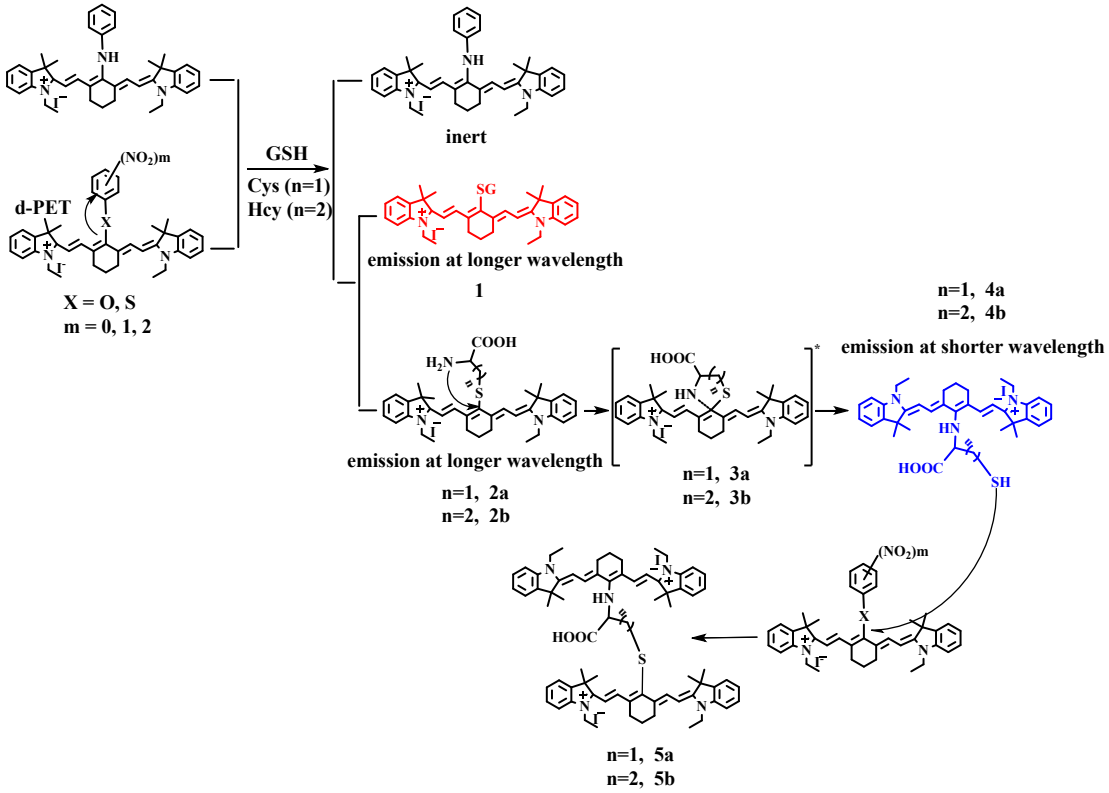

Figure S14. The proposed overall reaction mechanism of the synthesized NIR dyes towards biothiols.

15. Colocalization fluorescence images

The subcellular localization of Cy-3-NO_2 with Mito Tracker Green (Figure S15) gave a Pearson's correlation coefficient of 0.41, indicating that Cy-3-NO_2 does not localize to mitochondria.

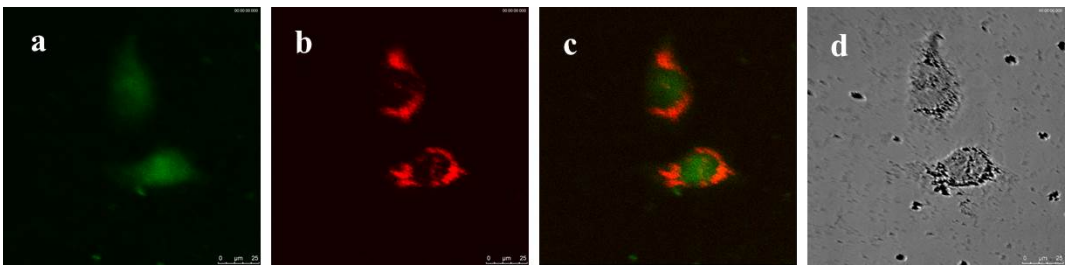

Figure S15. Colocalization fluorescence imaging of Cy-3-NO_2 in Hela cells. (a) Mito-Tracker Green (50 nM, λex=488 nm, collected in the range of 495–520 nm). (b) Cy-3-NO_2 (5 μM, λex =633 nm, collected in the range of 700–800 nm). (c) Merged images of (a) and (b). (d) Brightfield image. Scale bar = 25 μm.

Part II

1. The fluorescence spectra of Cy-Ph-Ph in the presence of biothiols

The FS monitoring revealed that in the tested GSH concentration range (0~1000 μM), the FI of Cy-Ph-Ph increased with increasing concentration of GSH, accompanied by a red shift of Em_{max} to 803 nm (Figure S16a). A good linearity between the FI and the GSH concentration in the range of 0.25-100 μM was observed (Fig. S17b). In the tested time period (0~120 min), the FI of Cy-Ph-Ph increased with increasing reaction times in the presence of GSH and the Em_{max} steadily red-shifted to 803 nm (Figure S16b).

The FS of Cy-Ph-Ph in the presence of Cys were recorded (Figure S18). As can be seen from Figure S18, the FI of Cy-Ph-Ph at 783 nm increased with Cys concentration up to 70 μM (Figure S18a). However, when more Cys was added, the FI did not rise but decreased and kept unchanged after addition of 700 μM Cys (Figure S18b). The dynamic investigation displayed an increase of Cy-Ph-Ph's FI within the first 20 min (Figure S19a). After that, the FI decreased along the reaction times (Figure S19b). As can be seen, no matter from the point of concentration and dynamics, the FS tend to return to where it was original.

In the case of Hcy, the FI of Cy-Ph-Ph increased with increasing Hcy concentration up to 500 μM, accompanied by a gradual red shift of Em_{max} to 797 nm. After that, the FS remained unchanged with more Hcy (Figure S20a). The dynamic examination exhibited a continuing increase of FI and a redshift of Em_{max} to 797 nm during the tested reaction period (0~120 min, Figure S20b). Compared with GSH, the FS variation caused by both Cys and Hcy during the experimental period can be neglectful.

To further testify the specific response of Cy-Ph-Ph to GSH, the FI of Cy-Ph-Ph at 803 nm (Em_{max}) was monitored in the presence of GSH, Cys, and Hcy at different incubation times (Figure S21). From Figure S21, it can be concluded that Cy-Ph-Ph possessed the highest *S*/*N* ratio for GSH and the influence from Cys/Hcy was tiny. So we expected that Cy-Ph-Ph would be a good candidate as an imaging probe for GSH in cells.

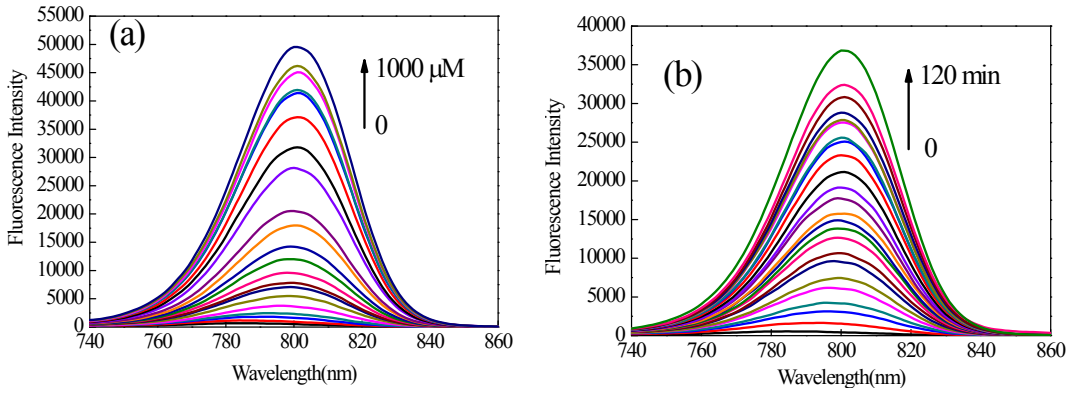

Figure S16. FS variation of Cy-Ph-Ph (10 μM) in the presence of GSH. (a) The FS recorded after Cy-Ph-Ph reacted with 0, 2.5, 5, 10, 20, 30, 50, 60, 70, 80, 100, 150, 200, 300, 400, 500, 600, 700, 800, 900, and 1000 μM GSH for 2h. (b) The FS recorded after Cy-Ph-Ph reacted with GSH (500 μM) for 0, 2.5, 5, 10, 15, 20, 25, 30, 45, 60, 70, 90, 100, 110, and 120 min. Experimental conditions: λ_{ex}=710 nm, 50 mM PBS buffer (pH=7.4, 1% CH_3CN), 37 °C.

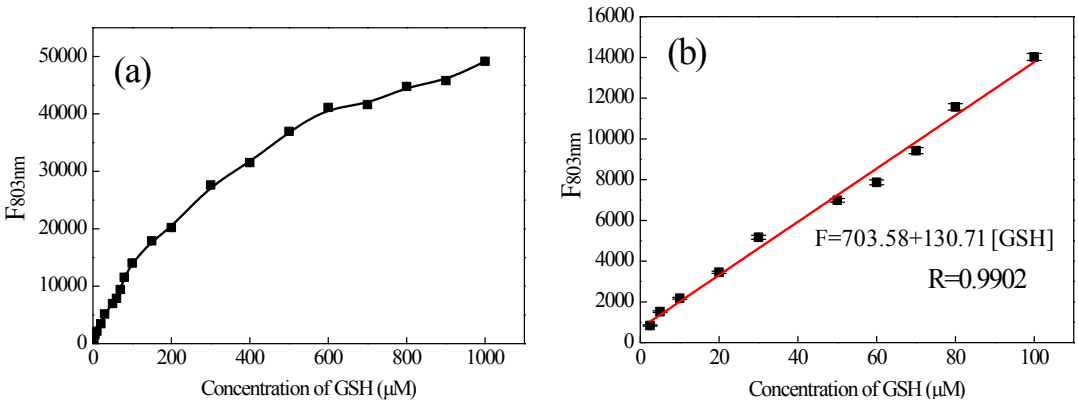

Figure S17. Dependence of FI of Cy-Ph-Ph (10 μM) upon different GSH concentrations. (a) FI of Cy-Ph-Ph with 0, 2.5, 5, 10, 20, 30, 50, 60, 70, 80, 100, 150, 200, 300, 400, 500, 600, 700, 800, 900, and 1000 μM GSH. (b) The linear relationship between FI of Cy-Ph-Ph and GSH concentrations. Experimental conditions: 50 mM PBS buffer (pH=7.4, 1% CH_3CN), 37 °C incubation for 2h, $\lambda_{ex}/\lambda_{ex}$=710/803 nm.

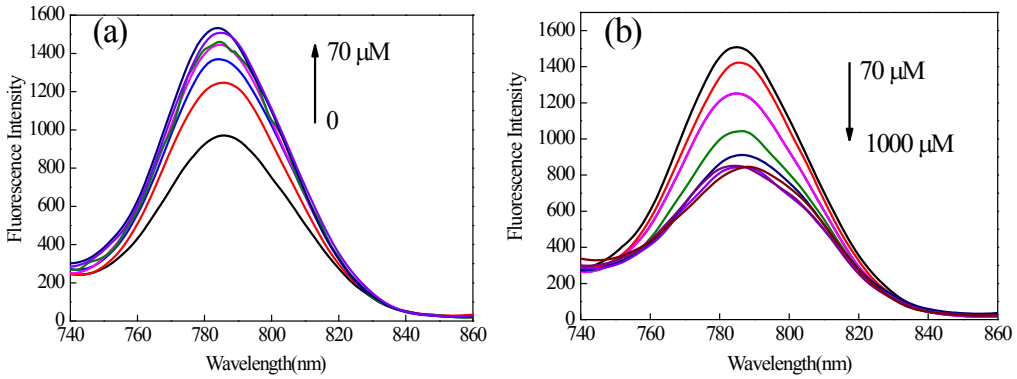

Figure S18. FS variation of Cy-Ph-Ph (10 μM) in the presence of different concentrations of Cys. (a) 0, 5, 10, 20, 30, 40, and 50 μM Cys. (b) 70, 100, 200, 300, 400, 500, 600,900, and 1000 μM Cys. Experimental conditions: λ_{ex}=710 nm, 50 mM PBS buffer (pH=7.4, 1% CH_3CN), 37 °C incubation for 2h.

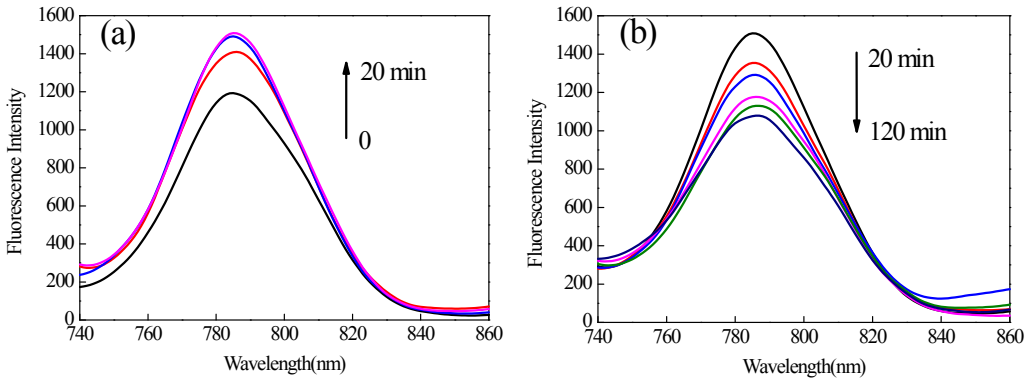

Figure S19. The FS recorded after Cy-Ph-Ph (10 μM) reacted with Cys (500 μM) for (a) 0, 5, 10, and 20 min and (b) 20, 30, 40, 60, 100, and 120 min. Experimental conditions: λ_{ex}=710 nm, 50 mM PBS buffer (pH=7.4, 1% CH_3CN), 37 °C.

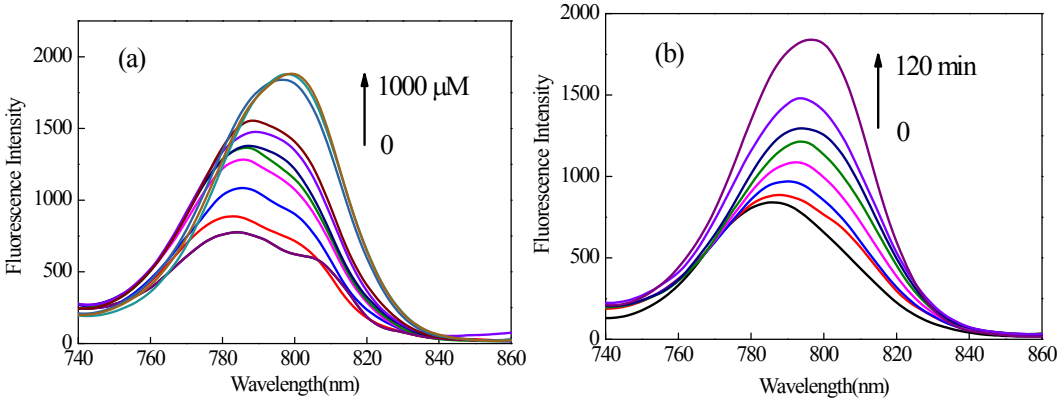

Figure S20. FS variation of Cy-Ph-Ph (10 μM) in the presence of Hcy. (a) The FS recorded after Cy-Ph-Ph reacted with 0, 5, 10, 20, 40, 60, 90, 100, 200, 500, 800, and 1000 μM Hcy for 2h. (b) The FS recorded after Cy-Ph-Ph reacted with Hcy (500 μM) for 0, 10, 20, 50, 70, 90, 110, and 120 min. Experimental conditions: λ_{ex}=710 nm, 50 mM PBS buffer (pH=7.4, 1% CH_3CN), 37 °C.

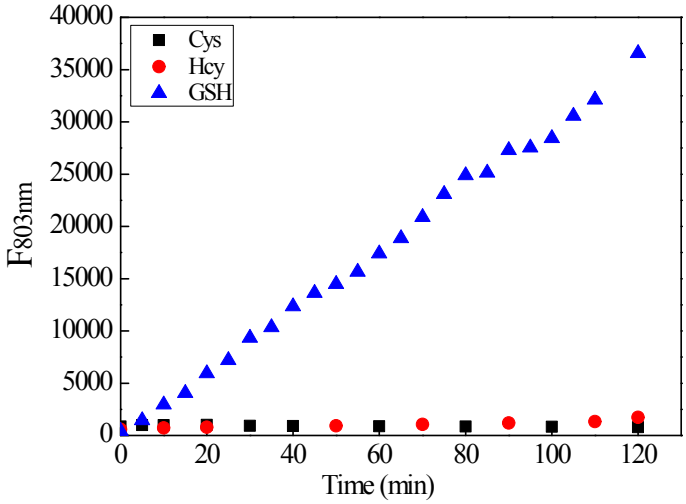

Figure S21. The dependence of FI of Cy-Ph-Ph (10 μM) in the presence of biological thiols (500 μM each) upon reaction times. Experimental conditions: $\lambda_{ex}/\lambda_{ex}$=710/803 nm, 50 mM PBS buffer (pH=7.4, 1% CH_3CN), 37 °C.

To gain a better insight into the mechanism of high specificity of Cy-Ph-Ph to GSH, density function theory (DFT) calculations were used to optimize the structures of compounds of Table 1 (not included Cy-GSH, Cy-Cys, and Cy-Hcy) at the B3LYP/6-31G(d) level, using a suite of Gaussian 09 programs. The results (Table S1) of the calculations show that the bond order of Cy-Ph-Ph (0.9146) is apparently smaller than that of Cy-3-NO_2 (0.9230), meaning its easier attack by sulfydryl. But Cy-Ph-Ph only showed unique specificity to GSH. We think the unique structure of NHNB could be the main source determining the reactivity towards GSH. NHNB holds one amide unit and one nitro group, and GSH contains two amides and one primary amine and has longer molecular skeleton in comparison to Cys and Hcy.[5]

Therefore, intermolecular hydrogen bond (for example N-H----O), may form between Cy-Ph-Ph and GSH. Moreover, the electrostatic interaction between the indolium cation of Cy-Ph-Ph and the carbonate anion of GSH may be another reason contributing to the mutually close interaction.[5] All of these intermolecular interactions will result in a closer distance of the two reactive sites (SH group and C-O group), resulting in a higher reactivity towards GSH. Figure S22 gives the probable interaction between Cy-Ph-Ph and GSH.

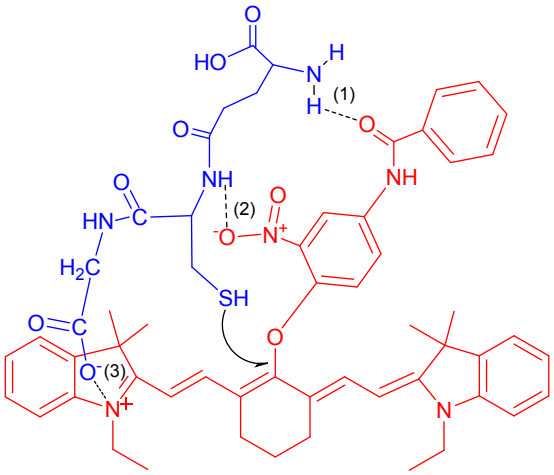

Fig. S22. The probable conformation of interaction between Cy-Ph-Ph and GSH. Interaction sites (1) and (2) denote hydrogen bond, and site (3) denotes electrostatic interaction.

2. Effect of pH on sensing behavior of Cy-Ph-Ph

The investigation on pH (Figure S23) showed that Cy-Ph-Ph are stable enough in a relatively wide pH range of 6.5-9.0, and display the obvious response for biothiols at pH 7.4.

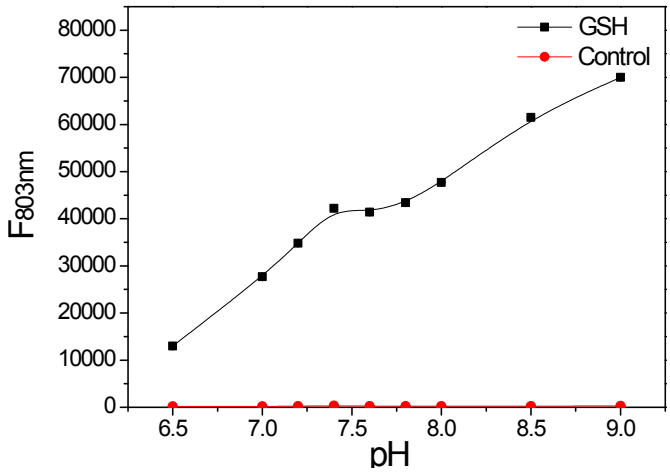

Figure S23. Effect of pH on the reaction of Cy-Ph-Ph and GSH ($\lambda_{ex/em}$=710/803 nm). The concentrations of probes and tested biothiols were 10 μM and 500 μM, respectively. 50 mM PBS buffer (pH=7.4, 1% CH_3CN), 37 ºC incubation for 2h.

3. Selectivity investigation of Cy-Ph-Ph

To evaluate the specific response of Cy-Ph-Ph to GSH, various species were examined in parallel under the same conditions, including amino acids, glucose, GSSG, ascorbic acid, H_2O_2, NO, and NO_2^- (Figure S24). It can be seen that the fluorescence of Cy-Ph-Ph showed significant enhancement upon reaction with GSH, while the fluorescence variations induced by other bio-substances was neglectable. These results suggest that Cy-Ph-Ph is highly selective for the targeting biothiols.

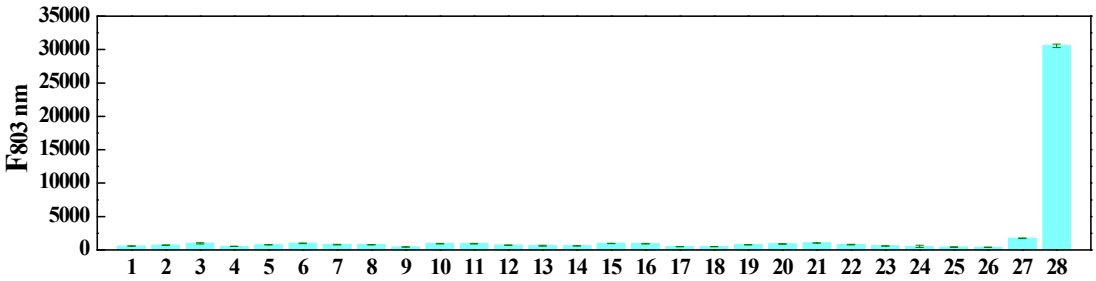

Figure S24. Fluorescence intensity changes of Cy-Ph-Ph (10 μM, $\lambda_{ex/em}$=710/803 nm) upon addition of various amino acids and biologically related substances after 2h in 50 mM PBS buffer (pH=7.4, 1% CH_3CN) at 37 ºC. (1) probe only, (2) Gly, (3) Ala, (4) Arg, (5) Asn, (6) Asp, (7) Gln, (8) Glu, (9) His, (10) Val, (11) Leu, (12) Lys, (13) Met, (14) Pro, (15) Ser, (16) Thr, (17) Trp, (18) Tyr, (19) Ile, (20) Glucose (500 μM), (21) Ascorbic acid (500 μM), (22) GSSG (500 μM), (23) NO (250 μM), (24) NO_2^- (500 μM), (25) H_2O_2 (500 μM), (26) Cys (500 μM), (27) Hcy (500 μM), (28) GSH (500 μM). The concentrations of the tested amino acids were all 500 μM.

4. HPLC-MS spectra of Cy-Ph-Ph

We investigated the interaction between Cy-Ph-Ph and the tested biothiols by HPLC-HRMS, intending to explain its high specificity to GSH. The HPLC chromatogram of Cy-Ph-Ph showed a peak at 20.9 min (Figure S25a), while that of mixture solution of Cy-Ph-Ph and GSH gave a new peak at 11.6 min (Figure S25b). When applied to MS analysis, the peaks at 11.6 and 20.9 min possessed m/z of 391.19 and 366.69, assigning to compound **1** and unreacted Cy-Ph-Ph, respectively (Figure S25c). However, in the presence of Cys (Figure S26) or Hcy (Figure S27), no apparent peak was found except two tiny peaks at 59.1 min (Figure S26b) and at 33.3 min (Figure S27b), which were analyzed and found no information. The results suggested that Cy-Ph-Ph is not so active to Cys and Hcy, which is accorded with the results from fluorescence analysis (Figure S2e).

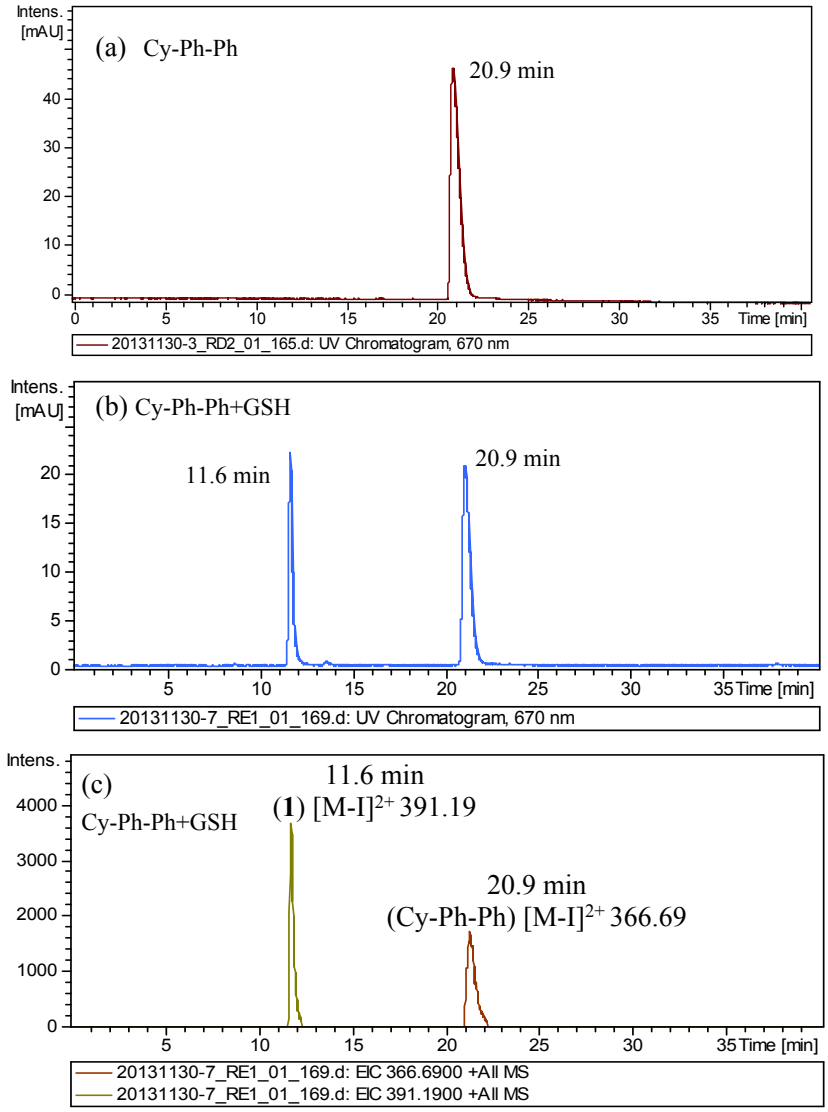

Figure S25. HPLC-HRMS spectra of Cy-Ph-Ph in the presence of GSH. Cy-Ph-Ph (10 μM) was incubated with 500 μM GSH in a 50 mM PBS buffer (pH=7.4) at 37 °C for 2h. Then the solution was applied to the chromatographic separation and analysed. (a) Cy-Ph-Ph only, (b) Cy-Ph-Ph + GSH, (c) MS analysis of (b). Eluant of HCOOH (1‰): methanol=20:80.

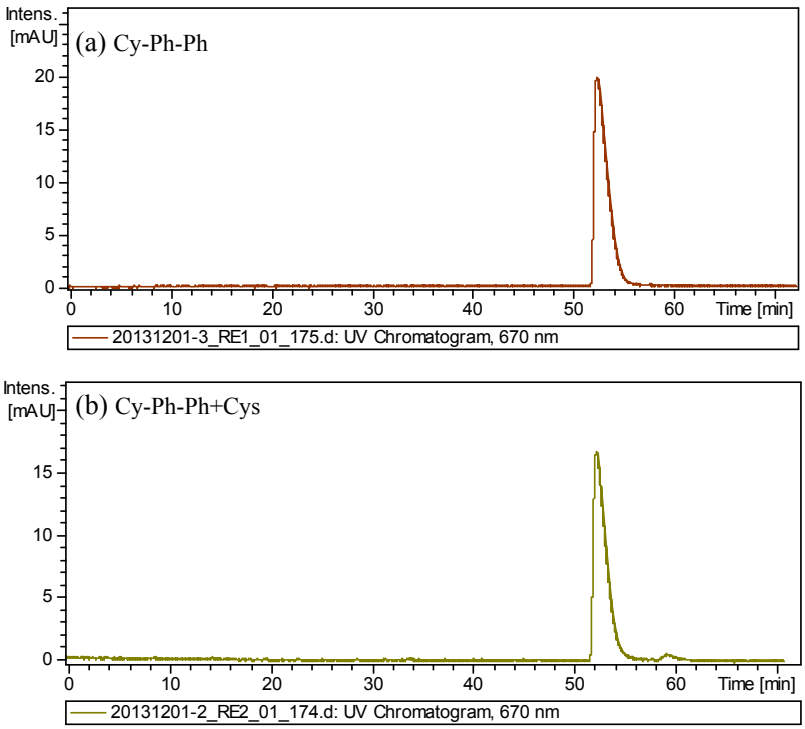

Figure S26. HPLC spectra of Cy-Ph-Ph in the presence of Cys. Cy-Ph-Ph (10 μM) was incubated with 500 μM Cys in a 50 mM PBS buffer (pH=7.4) at 37 °C for 2h. Then the solution was applied to the chromatographic separation. (a) Cy-Ph-Ph only, (b) Cy-Ph-Ph + Cys. Eluant of HCOOH (1‰): methanol=25:75.

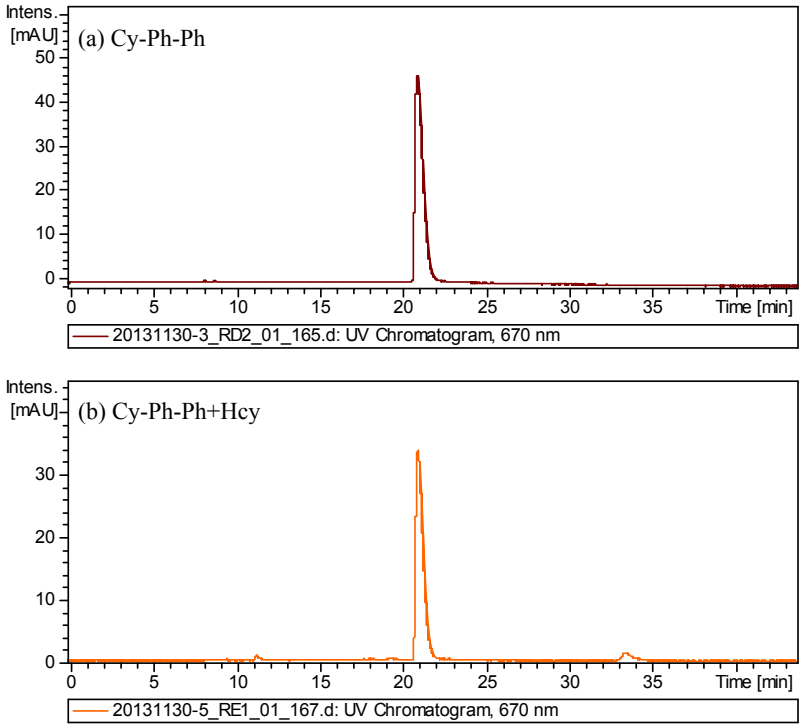

Figure S27. HPLC spectra of Cy-Ph-Ph in the presence of Hcy. Cy-Ph-Ph (10 μM) was incubated with 500 μM Hcy in a 50 mM PBS buffer (pH=7.4) at 37 °C for 2h. Then the solution was applied to the chromatographic separation. (a) Cy-Ph-Ph only, (b) Cy-Ph-Ph + Hcy. Eluant of HCOOH (1‰): methanol=20:80.

5. Confocal fluorescence images of Cy-Ph-Ph

After Hela cells were incubated with 5 μM Cy-Ph-Ph for 15 min, strong red fluorescence was observed (Figure S28), indicating good cell membrane permeability of Cy-Ph-Ph. Then a control experiment was performed by first removing intracellular thiols using 1 mM N-methylmaleimide (NEM, a thiol-blocking reagent)[6] and then incubating with 5 μM Cy-Ph-Ph. A marked fluorescence quenching was observed (Figure S28e), indicating that Cy-Ph-Ph could be applied for GSH imaging in living systems.

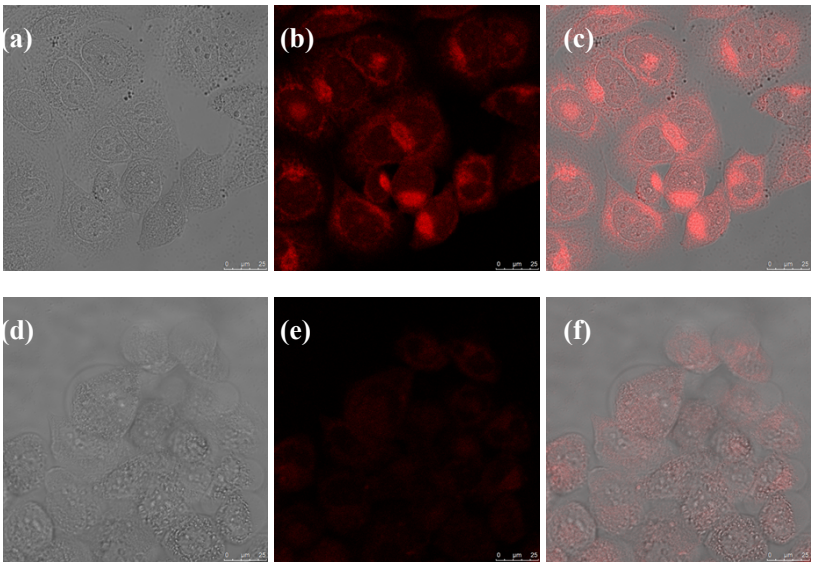

Figure S28. Confocal fluorescence images of GSH in Hela cells by Cy-Ph-Ph. (b) Hela cells were incubated with 5 μM Cy-Ph-Ph for 15 min. (e) The cells were first incubated with NEM for 30 min, then incubated with 5 μM Cy-Ph-Ph for 15 min. (a) and (d) Brightfield images of cells in (b) and (e). (c) and (f), merging of bright field images and dark field images. Images were obtained with band path of 700-800 nm upon 633 nm excitation. 37 ^{o}C, scale bar = 25 μm.

References

1 B. Tang, L. Zhang and K. H. Xu, *Talanta*, 2006, **68**, 876-882.

2 (a) X. Wang, J. Sun, W. H. Zhang, X. X. Ma, J. Z. Lv and B. Tang, *Chem. Sci.*, 2013, **4**, 2551-2556; (b) Z. Q. Guo, S. W. Nam, S. Park and J. Yoon, *Chem. Sci*., 2012, **3**, 2760–2765.

3 E. Sasaki, H. Kojima, H. Nishimatsu, Y. Urano, K. Kikuchi, Y. Hirata, T. Nagano, *J. Am. Chem. Soc.,* 2005, **127**, 3684-3685.

4 The calculations were carried out using Gaussian 09. The molecules were optimized in the gas phase at B3LYP/6-31G(d) level. Harmonic frequency analysis calculations were performed at the same level to verify the optimized structures to be minima.

Cite this work as:
Gaussian 09, Revision B.01,
M. J. Frisch, G. W. Trucks, H. B. Schlegel, G. E. Scuseria,
M. A. Robb, J. R. Cheeseman, G. Scalmani, V. Barone, B. Mennucci,
G. A. Petersson, H. Nakatsuji, M. Caricato, X. Li, H. P. Hratchian,
A. F. Izmaylov, J. Bloino, G. Zheng, J. L. Sonnenberg, M. Hada,
M. Ehara, K. Toyota, R. Fukuda, J. Hasegawa, M. Ishida, T. Nakajima,
Y. Honda, O. Kitao, H. Nakai, T. Vreven, J. A. Montgomery, Jr.,
J. E. Peralta, F. Ogliaro, M. Bearpark, J. J. Heyd, E. Brothers,
K. N. Kudin, V. N. Staroverov, R. Kobayashi, J. Normand,
K. Raghavachari, A. Rendell, J. C. Burant, S. S. Iyengar, J. Tomasi,
M. Cossi, N. Rega, J. M. Millam, M. Klene, J. E. Knox, J. B. Cross,
V. Bakken, C. Adamo, J. Jaramillo, R. Gomperts, R. E. Stratmann,
O. Yazyev, A. J. Austin, R. Cammi, C. Pomelli, J. W. Ochterski,
R. L. Martin, K. Morokuma, V. G. Zakrzewski, G. A. Voth,
P. Salvador, J. J. Dannenberg, S. Dapprich, A. D. Daniels,
O. Farkas, J. B. Foresman, J. V. Ortiz, J. Cioslowski,
and D. J. Fox, Gaussian, Inc., Wallingford CT, 2010.

5 J. Yin, Y. Kwon, D. Kim, D. Lee, G. Kim, Y. Hu, J. H. Ryu and J. Yoon, *J. Am. Chem. Soc.*, 2014, **136**, 5351-5358.

6 C. Yellaturu, M. Bhanoori and I. Neeli, *J Biol. Chem*., 2002, **277**, 40148-40155.